nature geoscience

ARTICLES

PUBLISHED ONLINE: 9 OCTOBER 2011 | DOI: 10.1038/NGEO1283

Arsenic migration to deep groundwater in Bangladesh influenced by adsorption and water demand

K. A. Radloff[1,2*†], Y. Zheng[2,3], H. A. Michael[4], M. Stute[2,5], B. C. Bostick[2], I. Mihajlov[2], M. Bounds[5], M. R. Huq[6], I. Choudhury[6], M. W. Rahman[3], P. Schlosser[1,2], K. M. Ahmed[6] and A. van Geen[2]

The consumption of shallow groundwater with elevated concentrations of arsenic is causing widespread disease in many parts of South and Southeast Asia. In the Bengal Basin, a growing reliance on groundwater sourced below 150-m depth—where arsenic concentrations tend to be lower—has reduced exposure. Groundwater flow simulations have suggested that these deep waters are at risk of contamination due to replenishment with high-arsenic groundwater from above, even when deep water pumping is restricted to domestic use. However, these simulations have neglected the influence of sediment adsorption on arsenic migration. Here, we inject arsenic-bearing groundwater into a deep aquifer zone in Bangladesh, and monitor the reduction in arsenic levels over time following stepwise withdrawal of the water. Arsenic concentrations in the injected water declined by 70% after 24 h in the deep aquifer zone, owing to adsorption on sediments; concentrations of a co-injected inert tracer remain unchanged. We incorporate the experimentally determined adsorption properties of sands in the deep aquifer zone into a groundwater flow and transport model covering the Bengal Basin. Simulations using present and future scenarios of water-use suggest that arsenic adsorption significantly retards transport, thereby extending the area over which deep groundwater can be used with low risk of arsenic contamination. Risks are considerably lower when deep water is pumped for domestic use alone. Some areas remain vulnerable to arsenic intrusion, however, and we suggest that these be prioritized for monitoring.

Elevated groundwater As concentrations are common within the upper 100 m of aquifer systems throughout South and Southeast Asia[1,2]. With the exception of its westernmost portion in the Indian state of West Bengal and the Sylhet Basin of Bangladesh, the As content of groundwater in the Bengal Basin at depths greater than 150 m is mostly $<10\,\mu g\,l^{-1}$, the World Health Organization's (WHO) drinking water guideline value[2–4]. In Bangladesh, the installation of more than 100,000 deep wells that are low in As (refs 3,5,6) has helped lower As exposure, but the vast majority have not been monitored over time[7]. At the same time, withdrawals for the municipal supply of large cities and concerns about the prolonged use of high-As water for irrigation[8] have increased demand for deeper groundwater[9]. Recent surveys of deep (>150 m) hand-pumped wells have shown that a worrisome 14–18% of those in Bangladesh[3,10] and 25% of those in the four most contaminated districts of West Bengal[11] contain As at concentrations $>10\,\mu g\,l^{-1}$. The proportion of larger-scale public water supply systems drawing from deeper aquifers (>150 m) in West Bengal that do not meet the WHO guideline for As is even higher[12]. It is unknown to what extent these observations reflect localized failures due to poor well construction, naturally occurring groundwater As at depth or, more troubling, the broad-scale contamination of deep groundwater from shallow sources. Previous groundwater flow simulations indicate that widespread contamination of deep groundwater may result from deep pumping for irrigation and some areas may even become contaminated when pumping is only for domestic use[13]. The adsorption of As onto iron minerals present in the sediment[14–16] could impede As transport into the deeper aquifers from intruding shallow groundwater, but adsorption properties have not been well characterized for deeper sediments in Bangladesh under realistic conditions[17]. The present study provides *in situ* measurements of As adsorption and directly addresses concerns about broad-scale contamination by presenting a new spatially resolved estimate of the vulnerability of deep groundwater throughout the Bengal Basin.

Measuring As adsorption

Our study site (90.6° E, 23.8° N) is located in the fluvial floodplain of central Bangladesh. Here groundwater As concentrations are elevated within the shallow, grey sands, reaching $210\,\mu g\,l^{-1}$ at 38 m depth[18]. Below 50 m lie brown sands characteristic of partially reduced Fe oxides that are associated with very low ($<2\,\mu g\,l^{-1}$) As concentrations in groundwater[9]. There is no low-permeability clay layer separating the two layers. A distinguishing feature of this study is that As adsorption parameters in the low-As aquifer were determined from both *in situ* experiments and batch As adsorption experiments. *In situ* estimates were derived from push–pull tests, where low-As groundwater was pumped from the brown

[1]Department of Earth and Environmental Engineering, Columbia University, New York, New York 10025, USA, [2]Division of Geochemistry, Lamont-Doherty Earth Observatory, Palisades, New York 10964, USA, [3]School of Earth and Environmental Sciences, Queens College, City University of New York, Flushing, New York 11367, USA, [4]Department of Geological Sciences, University of Delaware, Newark, Delaware 19716, USA, [5]Department of Environmental Science, Barnard College, New York, New York 10027, USA, [6]Department of Geology, University of Dhaka, Dhaka 1000, Bangladesh. †Present address: Gradient Corporation, Cambridge, Massachusetts 02138, USA. *e-mail: kradloff@gradientcorp.com.

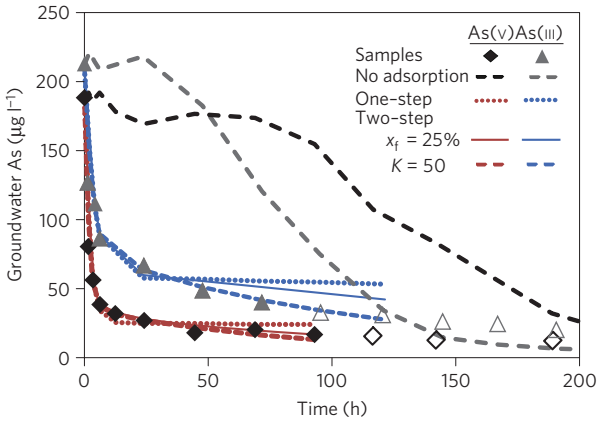

Figure 1 | Arsenic adsorption in push–pull tests. The rapid adsorption of As followed by a slow decrease towards equilibrium is observed in the As(v) and As(III) push–pull tests. In 24 h, 70% of As(III) and 85% of As(v) were adsorbed with most of the remaining As adsorbing over 200 h. Dashed lines indicate [As] if there was no adsorption (determined from [Br]). Samples with significant dilution (for example $[Br]/[Br]_0 < 0.85$) are shown as open symbols and were not used for model fitting. Best fits are shown for three scenarios—the one-step model, and a pair of two-step models based on the batch results (one where x_f was set to 25% and the other where the As(v) K was set to 50 l kg^{-1}).

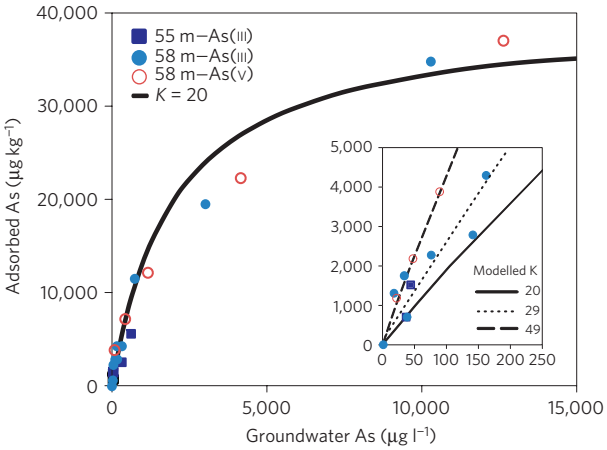

Figure 2 | Arsenic adsorption in batch isotherm experiments. Groundwater spiked with As(III) or As(v) was mixed with cuttings from the brown aquifers and sampled 145 h later. The solid line indicates the best fit sorption isotherm for brown sediments over the entire range of additions (up to 32,000 μg l^{-1}), whereas the dashed lines are best fits for As(III) or As(v) additions up to 3,000 μg l^{-1} (29 and 49 l kg^{-1}, respectively). The capacity of the brown sediment at 58 m is 40,000 μg kg^{-1}.

sands and immediately injected into a nearby well at the same depth after adding ~200 μg l^{-1} of As(III) or As(v) and bromide as a conservative tracer. The extent and rate of adsorption of both As species onto aquifer sands was determined by stepwise pumping of the injected water and measuring its loss of As over nine days. Concentrations of Br remained near the level of the injection for several of the withdrawals during the first two days of the experiment (Fig. 1). In contrast, concentrations of As(v) and As(III) dropped markedly within the first day, to 14% and 31% of their initial level, respectively, and declined further during subsequent days.

Batch experiments were conducted to support the field experiments by further characterizing adsorption of As(III) and As(v) using sands and groundwater from the same brown aquifer. The sorption capacity of brown sands freshly collected from drill cuttings is very high (40,000 μg kg^{-1}) and follows a Langmuir isotherm (Fig. 2). The resulting adsorption constant, K, is therefore effectively equal to the more commonly used partitioning coefficient, K_d(l kg^{-1}), given by the ratio of adsorbed As to dissolved As at equilibrium. Over the entire range of As additions up to 32,000 μg l^{-1}, the mean K for both As(III) and As(v) is 20 l kg^{-1}, and somewhat higher at concentrations below 3,000 μg l^{-1} (~30 and 50 l kg^{-1} for As(III) or As(v), respectively, Fig. 2). Measurement of adsorption over time indicates that rapid adsorption was followed by a slower approach to equilibrium (Supplementary Information). The result is best described by rapid adsorption for ~ 25% of the sites (x_f) and 50 times slower adsorption for the remaining sites. Similar two-step sorption behaviour has been observed for As in other systems[19–21].

A simple model that takes into account the spatial distribution of the injected As in groundwater and aquifer sands is required to relate batch adsorption parameters to the push–pull experiments. This model assumes homogeneous plug flow and Langmuir adsorption, and accounts for the stepwise withdrawal (Supplementary Information). Standard analytical solutions are not appropriate as they assume continuous pumping[22,23]. The field experiments indicate a conservative range of K_d values from 1 to 10 l kg^{-1}, whereas the batch experiments provide an upper limit for As adsorption that may occur given sufficiently slow flow conditions. The most conservative approach for estimating *in situ* As adsorption is to assume that all adsorption sites are equally accessible ($x_f = 100\%$), which results in K values of 1.8 l kg^{-1} for As(v) and 0.5 l kg^{-1} for As(III). This model does not fit the data well beyond the second day of the experiment ($r^2 = 0.94$ and 0.87, Fig. 1). Alternatively, two-step adsorption can be assumed by applying the two batch-derived adsorption parameters, $x_f = 25\%$ or $K = 50$ l kg^{-1}. When x_f is set to 25%, the resulting K values are 5.1 l kg^{-1} for As(v) and 1.7 l kg^{-1} for As(III) ($r^2 = 0.97$ and 0.96, Fig. 1); these values are much lower than observed in the batch experiments (Supplementary Table S8). When K is set to 50 l kg^{-1}, the high-end estimate from the As(v) batch experiments, the best model fit is achieved when $x_f = 3\%$ and slow adsorption sites comprised 97% of the total adsorption sites ($r^2 = 0.97$, Fig. 1), modestly higher than the fraction of less accessible adsorption sites in other heterogeneous flood plain aquifers (70–90%) that have been attributed to the presence of fine material, weathering and sand compaction[24,25]. When applying this x_f to the As(III) push–pull experiment, the calculated K is 13 l kg^{-1} ($r^2 = 0.99$, Fig. 1), which approaches the As(III) batch K of 30 l kg^{-1}. Taken together, the lower x_f and K values estimated here suggest that the limited duration and relatively rapid flow induced during the push–pull tests limited adsorption in comparison with the shaken slurries used in the batch experiments. Similar high adsorption estimates in batch studies (K_d values ranging from 35 to 70 l kg^{-1}; refs 17,26) and lower estimates derived indirectly from field observations (K_d values ranging from 1 to 4 l kg^{-1}; ref. 27) have been observed in multiple locations.

Sediment mineralogy considerably affects As adsorption and thus aquifer protection. The distribution of oxidized brown and reduced grey sediments associated with low-As, deep groundwater in the Bengal Basin is variable and not well documented[9,10,28]. Batch studies of shallow, high-As grey sediment indicate K_d values between 1 and 6 l kg^{-1} (refs 2,29,30; see also Supplementary Information), although a push–pull test carried out in high-As grey sands suggests that little As adsorption may occur above a concentration of 100 μg l^{-1} (ref. 31). Infiltration of reducing shallow groundwater may also result in the reduction of Fe oxyhydroxides (converting brown sands to grey) and the potential release of bound As[26,32], however these mechanisms are probably secondary

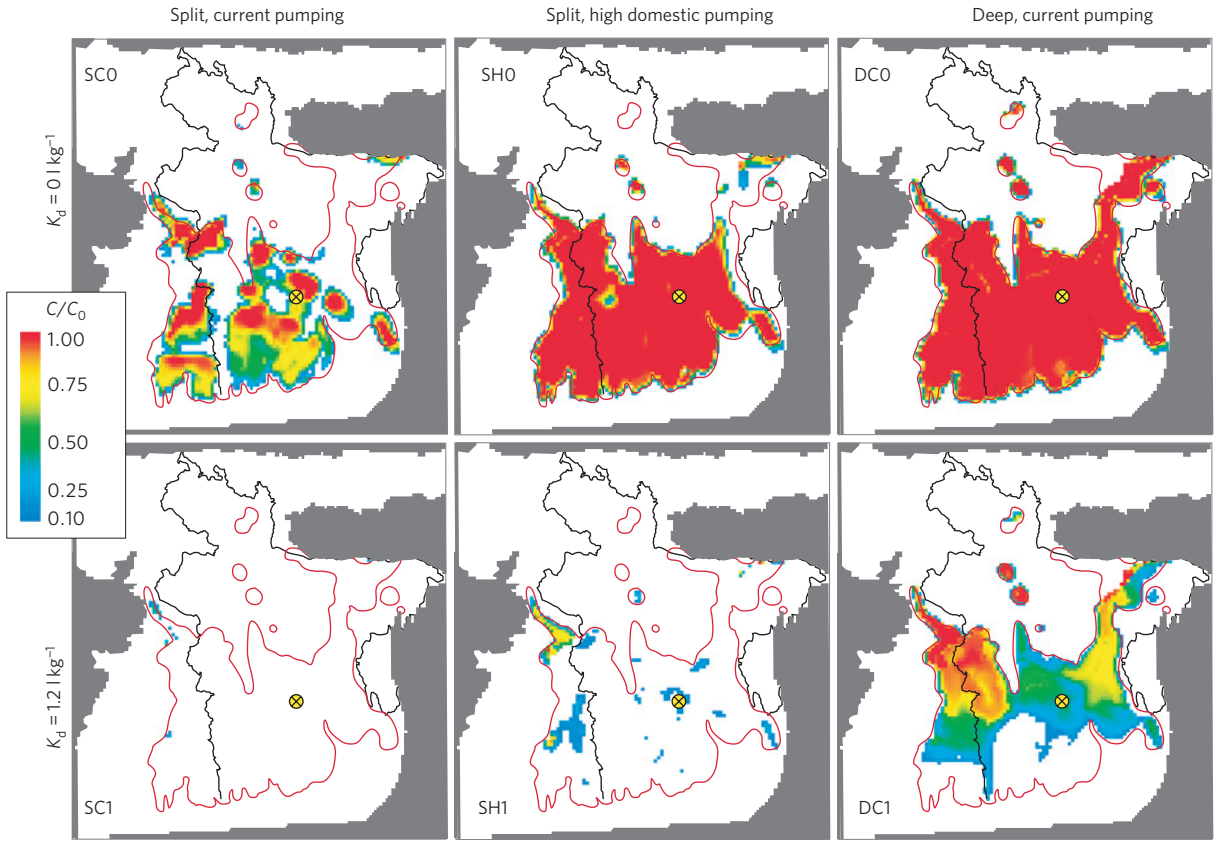

Figure 3 | Areas where deep, low-As groundwater is at risk of contamination. Model boundary is enclosed in grey, Bangladesh border is black, and red lines encircle regions with high-As groundwater in shallow aquifer zones[2,13]. Colour scale indicates simulated [As] for $C/C_0 > 0.1$ after 1,000 yr at a depth of 162 m. Modelled [As] is shown for the three water-use scenarios (SC, SH and D)—'split' with shallow irrigation and deep domestic pumping at current (50 l d^{-1} person^{-1}, SC) or future (200 l d^{-1} person^{-1}, SH) rates or 'deep' pumping only (DC) with two retardation factors ($K_d = 0$ and 1.2 l kg^{-1}). Yellow dot indicates the location of plotted concentrations in Fig. 4.

to adsorption. Given the likely lower adsorption on deeper grey sediments, we conservatively assume that the lower adsorption ($K_d \sim 1$) is characteristic of the majority of the deeper aquifer zones, although the spatial distribution of sorption parameters is unknown at present.

Basin-scale modelling of As transport

The adsorption properties of aquifer sands determined experimentally are incorporated into transport models to identify regions of the Bengal Basin most at risk of contamination. The MODFLOW-based advective flow model of Michael and Voss[13,33,34] was modified to include advective-dispersive solute transport and linear As adsorption (K_d) by using MT3DMS (refs 35,36), allowing for the calculation of As concentrations and depth-variable sorption. Within the source region where groundwater As concentrations are elevated in shallow aquifers[2,13], the initial concentration is constant ($C_0 = 1$) in the upper 50 m. Sorption is simulated only at depths >95 m, with retardation factors of 14 and 130 representing K_d values of 1.2 and 12 l kg^{-1}, which correspond to the average of the most conservative estimates of As(III) and As(V) adsorption from the push–pull experiments and one greater order of magnitude. We consider pumping from deep aquifers to be unsustainable (that is, at risk of contamination) when predicted As exceeds 10% of the upper aquifer concentrations in <1,000 years at 162 m depth (that is, when $C/C_0 > 0.1$ is 12 m below the top of the deeper pumping zone). In the district with the highest average As concentration in shallow groundwater[2], the threshold would be reached on average at 37 μg l^{-1}. The time span considered is longer than the practical management scale, but this allows for uncertainty and variability in local geochemical and hydrogeologic conditions.

Our adsorption experiments indicate that deeper sediments have a K_d of at least 1 l kg^{-1}. The protective effect of this weak As adsorption in comparison with the no-adsorption scenario (K_d of 0 l kg^{-1}) is illustrated with maps of $C/C_0 > 0.1$ after 1,000 years within the deep pumping zone (Fig. 3). Three water-use scenarios were simulated using the domestic and irrigation pumping rates of Michael and Voss[33]. Pumping rates were distributed based on district population and irrigation extents; estimated total irrigation pumping is ten times present domestic pumping rates (0.210 m yr^{-1} compared with 0.019 m yr^{-1}; ref. 33). Shallow domestic pumping was simulated from 10 to 50 m, shallow irrigation pumping from 50 to 100 m, and deep pumping from 150 to 200 m depth. In the two 'split' scenarios (S), irrigation pumping is shallow, whereas domestic pumping is deep with an estimated present rate of 50 l person^{-1} d^{-1} (refs 33,37) (SC) and a possible future rate of 200 l person^{-1} d^{-1} (SH), which was based on a quadrupling of present usage and is in line with the average domestic usage in Asia in 2000 (171 l person^{-1} d^{-1}; ref. 37). In the 'deep' scenario, both irrigation and domestic pumping are deep and at current rates (DC). In the 'split' pumping scenario with current domestic usage (SC), adsorption increases the area with sustainable deeper, low-As groundwater from 44% (SC0) of the affected region without retardation to 99% (SC1) with weak adsorption (Fig. 3). Even with high domestic water-use (SH), low-As water is still available for 91% of the high-As area when there is weak adsorption (SH1), but only for 16% of the area without As adsorption (SH0). Although As sorption is still protective in the 'deep' irrigation pumping

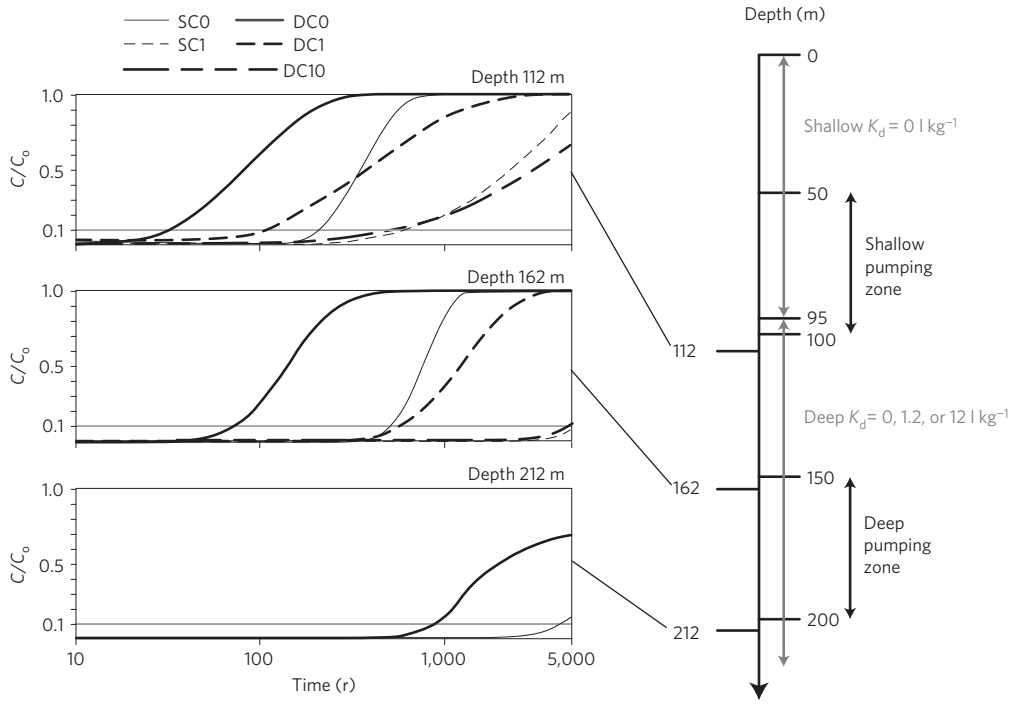

Figure 4 | Simulated groundwater [As] breakthrough by depth. [As] are simulated at three depths for one highly vulnerable location (indicated in Fig. 3) under the current 'split' pumping (SC) and the deep pumping (DC) scenarios. Domestic pumping is simulated within a constant depth range (150–200 m). Breakthrough curves for no ($K_d = 0$ l kg^{-1}, solid), low ($K_d = 1.2$ l kg^{-1}, dashed) and high ($K_d = 12$ l kg^{-1}, long dashed) retardation are shown over 5,000 years in log scale at three depths: 112 m is near the top of the low-As aquifer zone, 162 m is in the deep pumping zone and 212 m is below it.

scenario (DC), the simulated area that is sustainable is significantly reduced, with only 8% of the area sustainable with no sorption (DC0) and 37% with weak sorption (DC1). Further simulations suggest that increasing K_d to 12 l kg^{-1}, which may be appropriate for some sediments based on our adsorption isotherms, adds a considerable measure of protection, with 100% of the affected area in the 'split' scenarios (SC10 and SH10) and 96% of the area in the 'deep' scenario (DC10) remaining low-As over time (Supplementary Information).

The results from physically and chemically homogeneous basin-scale simulations provide an understanding of the effects of pumping and sorption on overall flow and transport behaviour and indicate regional trends resulting from basin geometry. Quantitative inferences about specific locations require knowledge and incorporation of site-specific parameters and heterogeneity (see ref. 34 for more information). However, the simulations do suggest that some regions are particularly vulnerable to contamination solely on the basis of their location within the basin. Where the basin is shallow, the flow paths connecting the contaminated shallow aquifers to the deeper aquifer zones are short, thus making these areas more vulnerable. For example, simulated As concentrations are high in a portion of northern West Bengal and west-central Bangladesh in <1,000 years in the deep pumping scenario, even with adsorption (Fig. 3). Another concern is areas where long flow paths still originate within the high-As region and connect the shallow and deeper aquifers, as is found in south-central Bangladesh. Breakthrough of high-As water in these and other areas may also be due to factors that were not incorporated in the model, such as high-capacity pumping wells, improperly installed or broken well casings, and hydrogeologic and geochemical heterogeneity.

We investigate specifically the sensitivity of the SC1 scenario to local increases in vertical hydraulic conductivity caused by fewer than average horizontally oriented layers of fine-grained sediment. On the scale of the basin, vertical flow is increased and results in larger areas of contamination. For anisotropy values of 1,000:1 and 100:1, the areas where deep domestic pumping is estimated to be sustainable are reduced to 89% and 52%, respectively, compared with 99% for the standard model anisotropy of 10,000:1. Such low anisotropy is not likely to occur everywhere in the basin, but there are regions where low-permeability horizontal layers may be missing, including our study location[9]. This and other uncertainties motivated the conservative timescale and adsorption coefficients used in the modelling.

Monitoring and management

The depth at which wells are screened to access low-As groundwater depends on many factors, including cost and sediment lithology. Although some deep well installations have targeted the brown, oxidized sediment for their low-As groundwater[7,38], wells are often screened only a few metres into such oxidized sediments, despite a government recommendation to install wells below a clay layer. We illustrate the protective effect of greater sediment thickness with breakthrough curves at several depths (Fig. 4) at a specific location in central Bangladesh that is vulnerable to downward As migration. At this location, flow paths are downward and travel times are short in both the deep and split pumping scenarios (DC and SC). An intermediate depth of 162 m was used in the vulnerability maps (Fig. 3) and breakthrough occurs in <1,000 years for the no adsorption 'split' pumping scenario (SC0). Breakthrough is twice as fast when the depth into adsorbing sediments is reduced by 50 m, whereas increasing depth by 50 m delayed breakthrough by a factor of five (Fig. 4). When adsorption is included (SC1), the delay of breakthrough is even greater, with breakthrough occurring more than five times slower at 162 m than it does at 112 m. Drawing water from beyond the shallowest possible depth therefore offers considerably more protection against intrusion of shallow high-As water, but must be weighed against the increased installation and operation costs, greater drawdowns, and decreased water yields of deeper wells.

The combination of *in situ* field measurements with basin-scale modelling presented in this study shows that As adsorption on deeper sediments significantly impedes As migration, allowing for the provision of low-As drinking water to a majority of the As-affected areas of Bangladesh for the foreseeable future. This suggests that the high As concentrations observed in some isolated deep wells may not be the result of widespread contamination, but that well construction quality and naturally occurring groundwater As at depth must be considered as possible causes. Modelling indicates that greater withdrawals due to increased domestic use are unlikely to trigger contamination of deep groundwater by As in most of the Bengal Basin. Caution is needed, however, as piped water supplies for growing municipalities are developed, because this analysis considers only spatially distributed pumping by millions of hand pumps. High-capacity pumping wells could facilitate local deep groundwater contamination. Our results also indicate that most of the Bengal Basin is highly vulnerable to downward migration of high-As groundwater caused by increased withdrawals of deeper groundwater for irrigation, even with the protective effect of sorption. The use of low-As deep groundwater for irrigation should therefore be discouraged, particularly in the areas that are vulnerable to As contamination under domestic-only withdrawal scenarios (SC and SH). Because irrigating rice paddies with high-As groundwater can have adverse effects[8], alternative sources of irrigation water as well as farming less water-intensive crops should be considered. Our study highlights particular areas and pumping scenarios where the risk of downward migration of high-As groundwater is elevated. These findings can be used to prioritize both monitoring and water-use management of deeper aquifers. The many deep community wells now in use throughout the country clearly need to be tested periodically to prevent renewed exposure to As.

Methods summary

The As adsorption push–pull tests were conducted in two wells, for As(III) and As(V), using groundwater from a third well with a similar geochemical composition, and all were screened at 60 m (Supplementary Information). To limit the geochemical alteration of the groundwater, a concentrated solution of As and Br was dynamically added to ~1,000 l of low-As groundwater as it was pumped from the source well into the receiving well ~10 m away, such that the injected water contained ~200 $\mu g\,l^{-1}$ of As(III) or As(V) and ~50 $mg\,l^{-1}$ Br. An inflation packer (Solinst) was deployed to limit dilution within the well casing. Adsorption was monitored through 21 individual 'pulls' of 100 l over nine days.

The push–pull test using only Br employed two separate wells, screened at 65 m and 10 m apart, at the same location and injected 540 l of deep groundwater with 130 $mg\,l^{-1}$ of Br, followed by 80 l of groundwater without tracer. After two days, 910 l of groundwater was continuously pumped out.

Batch experiments were conducted on freshly collected drill cuttings and groundwater, and the slurries were prepared in the field under near anaerobic conditions within a few hours of collection. Adsorption isotherms were constructed with As additions ranging from 440 to 32,000 $\mu g\,l^{-1}$ and sampled after 145 h. Kinetic parameters were determined from monitoring a 3,000 $\mu g\,l^{-1}$ addition of As(III) over 400 h.

Arsenic adsorption was described using a Langmuir model with a single site type. The kinetics of adsorption was modelled by a two-step adsorption process in which a portion (x_f) of sites react rapidly with solution, whereas the rest of the sites ($1-x_f$) have equivalent reactivity but react more slowly, presumably because of diffusion. This division of sites could reflect differences in adsorption sites themselves or the physically restricted access to some sites because of intra-granular or immobile porosity. The push–pull experiments were modelled assuming homogeneous plug flow through concentric rings, each with 100 l of groundwater. Because the time between 'pulls' is large (from 1 to 24 h), the resting time was divided into 20 equal time steps. The simplification to plug flow is supported by a push–pull test at the same site using only the Br tracer that determined dispersivity in the aquifer was small, only 0.5 cm over the 70 cm radius penetrated by the tracer, and 90% of the injected Br was recovered when the injected volume was removed ($V = V_0$). For the longer duration push–pull experiments with As, >75% of the injected Br was recovered when $V = V_0$. Because our model neglects dispersion, we constrain our model fitting to the early part of the experiment, when samples were only marginally affected by these processes ($[Br]/[Br]_0 < 0.85$). The first sampling point was ignored because the concentrations are changing so rapidly that small timing differences at this point significantly altered the fit of the other data; the best parameter fit was achieved by minimizing the least squares differences between modelled and measured groundwater As concentrations. The sensitivity of model results to the box size was tested using a model with boxes one tenth in size and this did not substantially change results.

The Bengal Basin groundwater model was modified from the model of Michael and Voss[13,33,34]. Transport was simulated using an initial concentration ($C_0 = 1$) in the upper 50 m and a constant concentration of 1 at the ground surface as a normalized representation of variable As concentrations, of which average As concentration of districts within the affected region of Bangladesh range from 50 to 366 $\mu g\,l^{-1}$ (ref. 2). Model geometry and flow parameters, homogeneous over the basin, were identical to those estimated as the 'base case' model of Michael and Voss[34], with a horizontal hydraulic conductivity of 5×10^{-4} m s^{-1}, a vertical hydraulic conductivity of 5×10^{-8} m s^{-1}, and a porosity of 0.2. The longitudinal dispersivity value of 100 m was chosen as small as possible on the coarse (5 km × 5 km) grid while minimizing errors and preventing excessive simulation times; this value is consistent with literature values for systems with similar spatial scale[39,40]. Transverse dispersivity was 0.1 m in the horizontal direction and 0.01 m in the vertical direction. The sensitivity of model results to grid spacing and numerical solver was tested. Doubling the spatial discretization in the vertical and horizontal directions did not substantially change the results or improve convergence, although it should be noted that even 2.5 km × 2.5 km cells are very large compared with the scale of solute transport processes, so this regional study may exaggerate dispersion. The numerical solver that best minimized numerical dispersion and oscillation and mass balance errors in this case was a third order total-variation diminishing scheme (TVD solver, ref. 36).

Received 7 February 2011; accepted 8 September 2011; published online 9 October 2011

References

1. Ravenscroft, P., Brammer, H. & Richards, K. *Arsenic Pollution: A Global Synthesis* (Wiley-Blackwell, 2009).
2. BGS/DPHE (British Geological Survey, Dept. of Public Health Engineering). *Arsenic Contamination of Groundwater in Bangladesh*, Final Report (British Geological Survey, 2001).
3. BBS/UNICEF (Bangladesh Bureau of Statistics/United Nations Children's Fund) *Bangladesh National Drinking Water Quality Survey of 2009* (UNICEF, 2011).
4. Fendorf, S., Michael, H. A. & van Geen, A. Spatial and temporal variations of groundwater arsenic in south and southeast Asia. *Science* **328,** 1123–1127 (2010).
5. Ahmed, M. F. *et al.* Epidemiology: Ensuring safe drinking water in Bangladesh. *Science* **314,** 1687–1688 (2006).
6. DPHE/JICA (Dept. of Public Health Engineering, Bangladesh, Japan International Cooperation Agency) *Report on Situation Analysis of Arsenic Mitigation, 2009* (Local Government Division, Government of Bangladesh, DPHE, JICA, 2010).
7. van Geen, A. *et al.* Monitoring 51 community wells in Araihazar, Bangladesh, for up to 5 years: Implications for arsenic mitigation. *J. Environ. Sci. Health A* **42,** 1729–1740 (2007).
8. Brammer, H. & Ravenscroft, P. Arsenic in groundwater: A threat to sustainable agriculture in South and South-east Asia. *Environ. Int.* **35,** 647–654 (2009).
9. Zheng, Y. *et al.* Geochemical and hydrogeological contrasts between shallow and deeper aquifers in two villages of Araihazar, Bangladesh: Implications for deeper aquifers as drinking water sources. *Geochim. Cosmochim. Acta* **69,** 5203–5218 (2005).
10. Burgess, W. G. *et al.* Vulnerability of deep groundwater in the Bengal Aquifer System to contamination by arsenic. *Nature Geosci.* **3,** 83–87 (2010).
11. Chakraborti, D. *et al.* Status of groundwater arsenic contamination in the state of West Bengal, India: A 20-year study report. *Mol. Nutr. Food Res.* **53,** 542–551 (2009).
12. Mukherjee, A. *et al.* Elevated arsenic in deeper groundwater of the western Bengal basin, India: Extent and controls from regional to local scale. *Appl. Geochem.* **26,** 600–613 (2011).
13. Michael, H. A. & Voss, C. I. Evaluation of the sustainability of deep groundwater as an arsenic-safe resource in the Bengal Basin. *Proc. Natl Acad. Sci. USA* **105,** 8531–8536 (2008).
14. Dixit, S. & Hering, J. G. Comparison of arsenic(V) and arsenic(III) sorption onto iron oxide minerals: Implications for arsenic mobility. *Environ. Sci. Technol.* **37,** 4182–4189 (2003).
15. Jonsson, J. & Sherman, D. M. Sorption of As(III) and As(V) to siderite, green rust (fougerite) and magnetite: Implications for arsenic release in anoxic groundwaters. *Chem. Geol.* **255,** 173–181 (2008).
16. Smedley, P. L. & Kinniburgh, D. G. A review of the source, behaviour and distribution of arsenic in natural waters. *Appl. Geochem.* **17,** 517–568 (2002).
17. Stollenwerk, K. G. *et al.* Arsenic attenuation by oxidized aquifer sediments in Bangladesh. *Sci. Total Environ.* **379,** 133–150 (2007).
18. Radloff, K. A. *et al.* Mobilization of arsenic during one-year incubations of grey aquifer sands from Araihazar, Bangladesh. *Environ. Sci. Technol.* **41,** 3639–3645 (2007).

19. Fuller, C. C., Davis, J. A. & Waychunas, G. A. Surface-chemistry of Ferrihydrite. 2. Kinetics of arsenate adsorption and coprecipitation. *Geochim. Cosmochim. Acta* **57,** 2271–2282 (1993).
20. Raven, K. P., Jain, A. & Loeppert, R. H. Arsenite and arsenate adsorption on ferrihydrite: Kinetics, equilibrium, and adsorption envelopes. *Environ. Sci. Technol.* **32,** 344–349 (1998).
21. Selim, H. M. & Zhang, H. Arsenic adsorption in soils: Second-order and multireaction models. *Soil Sci.* **172,** 444–458 (2007).
22. Schroth, M. H., Istok, J. D. & Haggerty, R. *In situ* evaluation of solute retardation using single-well push–pull tests. *Adv. Water Resour.* **24,** 105–117 (2001).
23. Cassiani, G., Burbery, L. F. & Giustiniani, M. A note on *in situ* estimates of sorption using push–pull tests. *Wat. Resour. Res.* **41,** W03005 (2005).
24. Haggerty, R. & Gorelick, S. M. Multiple-rate mass-transfer for modeling diffusion and surface-reactions in media with pore-scale heterogeneity. *Wat. Resour. Res.* **31,** 2383–2400 (1995).
25. Wood, W. W., Kraemer, T. F. & Hearn, P. P. Intragranular diffusion—an important mechanism influencing solute transport in clastic aquifers. *Science* **247,** 1569–1572 (1990).
26. Dhar, R. K *et al*. Microbes enhance mobility of arsenic in Pleistocene aquifer sand from Bangladesh. *Environ. Sci. Technol.* **45,** 2648–2654 (2011).
27. McArthur, J. M. *et al*. Migration of As, and $^{3}H/^{3}He$ ages, in groundwater from West Bengal: Implications for monitoring. *Wat. Res.* **44,** 4171–4185 (2010).
28. Goodbred, S. L., Kuehl, S. A., Steckler, M. S. & Sarker, M. H. Controls on facies distribution and stratigraphic preservation in the Ganges–Brahmaputra delta sequence. *Sedim. Geol.* **155,** 301–316 (2003).
29. Jung, H. B., Charette, M. A. & Zheng, Y. Field, laboratory, and modeling study of reactive transport of groundwater arsenic in a coastal aquifer. *Environ. Sci. Technol.* **43,** 5333–5338 (2009).
30. van Geen, A. *et al*. Flushing history as a hydrogeological control on the regional distribution of arsenic in shallow groundwater of the Bengal Basin. *Environ. Sci. Technol.* **42,** 2283–2288 (2008).
31. Harvey, C. F. *et al*. Arsenic mobility and groundwater extraction in Bangladesh. *Science* **298,** 1602–1606 (2002).
32. Polya, D. & Charlet, L. Environmental science: Rising arsenic risk? *Nature Geosci.* **2,** 383–384 (2009).
33. Michael, H. A. & Voss, C. I. Controls on groundwater flow in the Bengal Basin of India and Bangladesh: Regional modeling analysis. *Hydrogeol. J.* **17,** 1561–1577 (2009).
34. Michael, H. A. & Voss, C. I. Estimation of regional-scale groundwater flow properties in the Bengal Basin of India and Bangladesh. *Hydrogeol. J.* **17,** 1329–1346 (2009).
35. Harbaugh, A. W., Banta, E. R., Hill, M. C. & McDonald, M. G. *MODFLOW-2000, the US Geological Survey Modular Ground-Water Model—User Guide to Modularization Concepts and the Ground-Water Flow Process* US Geological Survey Open-File Report 00–92 (US Department of the Interior, US Geological Survey, 2000).
36. Zheng, C. & Wang, P. P. *MT3DMS: A Modular Three-Dimensional Multispecies Model for Simulation of Advection, Dispersion and Chemical Reactions of Contaminants in Groundwater Systems; Documentation and User's Guide*. (US Army Engineer Research and Development Center, 1999).
37. Gleick, P. H. *et al*. *The World's Water: 2008–2009* (Island Press, 2009).
38. von Bromssen, M. *et al*. Targeting low-arsenic aquifers in Matlab Upazila, Southeastern Bangladesh. *Sci. Total Environ.* **379,** 121–132 (2007).
39. Gelhar, L. W., Welty, C. & Rehfeldt, K. R. A critical review of data on field-scale dispersion in aquifers. *Wat. Resour. Res.* **28,** 1955–1974 (1992).
40. Neuman, S. P. Universal scaling of hydraulic conductivities and dispersivities in geologic media. *Wat. Resour. Res.* **26,** 1749–1758 (1990).

Acknowledgements

Columbia University and the University of Dhaka's research in Araihazar has been supported since 2000 by NIEHS Superfund Basic Research Program grant NIEHS 5 P42 ES010349. Undergraduate student support was received from Barnard College and the Earth Institute at Columbia University. The authors thank L. Konikow and C. Voss (US Geological Survey) for modelling advice and H. C. Siu for the grain size analysis (Bronx Science High School). This is Lamont-Doherty Earth Observatory contribution number 7496.

Author contributions

K.A.R., Y.Z., M.S., K.M.A. and A.v.G. designed the adsorption studies. K.A.R., M.S., I.M. and Y.Z. conducted the push–pull experiments. Y.Z. conducted the batch adsorption experiments. H.M. designed and executed the hydrological model of the Bengal Basin. I.M., M.B., M.R.H., I.C., M.W.R. provided field and laboratory assistance for the adsorption experiments. B.C.B. provided sediment mineralogical analysis. P.S. advised and supported the work of K.A.R. K.A.R, Y.Z., and H.M. analysed the data and wrote the paper, which was then edited by A.v.G.

Additional information

The authors declare no competing financial interests. Supplementary information accompanies this paper on www.nature.com/naturegeoscience. Reprints and permissions information is available online at http://www.nature.com/reprints. Correspondence and requests for materials should be addressed to K.A.R.

nature geoscience

SUPPLEMENTARY INFORMATION

DOI: 10.1038/NGEO1283

Arsenic migration to deep groundwater in Bangladesh influenced by adsorption and water demand

K.A. Radloff, Y. Zheng, H.A. Michael, M. Stute, B. C. Bostick, I. Mihajlov, M. Bounds, M. R. Huq, I. Choudhury, M.W. Rahman, P. Schlosser, K. M. Ahmed, A. van Geen

Supplementary Methods

Batch adsorption experiments

The batch adsorption experiments were conducted on freshly collected drill cuttings and groundwater and were prepared in the field under near anaerobic conditions within a few hours of collection in a nitrogen-filled portable glove box (Bel-Art). Groundwater was collected from a nearby well (Table S1) and kept anoxic. Brown sediments were collected by traditional manual well drilling at 55 m and 58 m depth, and gray sediments at 40 m and 46 m depth (Table S2). In the batch isotherm (BI) experiment, Langmuir adsorption isotherms were constructed from As additions ranging from 440 to 32,000 μg L^{-1} and sampled after 145 hours (Table S3). Kinetic parameters were determined on sediment from 40 and 58 m by monitoring a 3,000 μg L^{-1} addition of As(III) over 400 hours, referred to as the batch kinetic (BK) experiments (Table S4). Groundwater As concentrations were altered in the batch experiments using an 1,000 mg L^{-1} As spike prepared from reagent grade $NaAsO_2$ or $NaHAsO_4 \cdot 7H_2O$.

As adsorption push-pull tests

Each push-pull test, one for As(III) and one for As(V), required a receiving well and the same source well was used for both tests. All wells were screened at ~ 60 m in the deep aquifer zone and had a similar geochemical composition (Table S1). The source well was pumped with a locally available irrigation pump at 12 L min^{-1}, while a high-pressure gradient piston pump

(Cole-Parmer) was used to introduce the concentrated As and Br solution at 2 mL min^{-1} into the source water. Approximately 1,000 litres of low-As groundwater was dynamically modified to contain ~200 μg L^{-1} of As(III) or As(V) and ~50 mg L^{-1} Br. This mixture was immediately injected into the receiving well to limit the geochemical alteration of the groundwater. An inflation packer (Solinst) was deployed at 45 m to limit dilution. For As(V), 1240 L of groundwater with 190 μg L^{-1} of As(V) and 40.0 mg L^{-1} of Br was injected into a well 9 m from the source well (Table S5). For As(III), 780 L of groundwater with 210 μg L^{-1} of As(III) and 55.5 mg L^{-1} of Br was injected into a well 11 m from the source well (Table S6). Adsorption was monitored through 21 pulls of 100 L over 9 days.

Bromide only push-pull test

Two separate wells, screened at 65 m and 10 m apart, at the same location were used for a Br only push-pull test. During this experiment, 540 L of deep groundwater dynamically mixed with Br and injected into the receiving well with a Br concentration of 130 mg L^{-1}. This injection was followed by 80 L of groundwater without tracer, to enhance dispersion. The tracer solution was allowed to rest in the aquifer for 2 days and then 907 L of groundwater was pumped out at one time (Table S7).

Field Measurements

Groundwater was continuously monitored for temperature, pH and conductivity using a multi-parameter water monitoring probe in a flow cell (MP 556 from YSI, Inc.). Dissolved oxygen (Chemetrics) and alkalinity were measured using standard methods [1], with As(III) and As(V) separation by a sorption-based cartridge [2].

Laboratory Analyses

Groundwater samples acidified to 1% HCl (Optima) were analyzed by High-Resolution Inductively Coupled Plasma Mass Spectrometry (HR ICP-MS) for As, Fe, Mn, S and P [3]. Supernatant from batch experiments were filtered through 0.45 μm syringe filters before HR ICP-MS analysis, with As(III) determined using differential pulse cathodic stripping voltammetry (DPCSV) [4,5]. Bromide was measured by ion chromatography (IC) [6].

Coarse fraction (sand) analysis separated the sediment into three size fractions: >150 μm, 63-150 μm, and <63 μm [7]. The porosity of the aquifer was assumed to be 0.25 with a bulk density of 2.65 g cm^{-3} based on the BGS characterization of the deeper aquifer [8]. Sediment from the batch isotherms underwent a sequential extraction to remove sorbed As using distilled water (24 hr), 1M phosphate (24 hr) and 1.2 N HCl (60 ^{o}C for 24 hrs). The samples from the extractions were then analyzed for As using an ICP-MS (Thermo, Waltham, MA) operating in the automated Collision Cell Technique (CCT) model [9]. Mn minerals were also measured in sediments that received either no or the largest As addition with x-ray absorption near edge spectroscopy (XANES) using standard methods [10].

Adsorption equations

The adsorption of As to sediment surface can be described using the Langmuir model as follows:

$$\frac{dS}{dt} = \frac{\theta}{\rho} k_f C\left(1 - \frac{S}{S_{\max}}\right) - k_r S \qquad \text{(eq. 1)}$$

where C is the dissolved concentration [μg L^{-1}], S is the sorbed concentration [μg kg^{-1}], S_{max} is the sorption capacity [μg kg^{-1}], θ is the porosity [L L^{-1}], ρ is the bulk density [kg L^{-1}], k_f

is the adsorption rate constant [hr^{-1}] and k_r is the desorption rate constant [hr^{-1}] [11]. At equilibrium, equation 1 becomes:

$$K = \frac{\theta}{\rho} * \frac{k_f}{k_r} = \frac{S}{C * (1 - \frac{S}{S_{\max}})} \qquad \text{(eq. 2)}$$

K [L groundwater kg^{-1} sediment] can be understood as similar to the partitioning coefficient K_d (defined as the ratio of sorbed As (S) to dissolved As (C)), but includes the adsorption capacity (S_{max}). At low concentrations when $S << S_{max}$, K_d is nearly identical to K.

The heterogeneity of sediment surfaces was treated as though one site was present, but that adsorption occurs first on the readily available, rapidly adsorbing sites (the "fast" sites) following eq. 1, and is then transferred by diffusion to the less available, "slow" adsorbing sites[12], thus there are two-steps of adsorption. Equation 1 was modified to include the transfer of sorbed As from the fast to the slow sites, represented by a simple diffusion reaction, thus the sorption on the fast sites can be described as:

$$\frac{dS_f}{dt} = \frac{\theta}{\rho} k_f C (1 - \frac{S_f}{S_{\max}}) - k_r S_f + \frac{k_{diff} * (S_s - S_f)}{x_f} \qquad \text{(eq. 3)}$$

where S_f is the sorbed concentration on the fast sites [µg kg^{-1}], S_s is the sorbed concentration on the slow sites [µg kg^{-1}], x_f is the fraction of fast to total sites [dimensionless], and k_{diff} is the rate of exchange from the fast to the slow sites [hr^{-1}]. The model assumes there is no difference in the sorption capacity (S_{max}) or equilibrium partitioning (K) between the two site types, so at equilibrium $S_f = S_s$. The As concentration on the slow sites is described as:

$$\frac{dS_s}{dt} = \frac{k_{diff} * (S_f - S_s)}{1 - x_f} \qquad \text{(eq. 4)}$$

Model for push-pull experiments

A simple model was constructed to implement the sorption reactions described in equations 3 and 4 during the injection (push) and extraction (pull) phases of the experiments. Common analytical approaches [13,14] to modelling such tests were not possible since the pull was conducted step-wise, with brief periods of pumping for sampling followed by gradually longer intervals of rest. This model tracks the concentrations of dissolved As and sorbed As on fast and slow sites in discrete, equal volume rings surrounding the well. The concentric rings were composed of 100 L of groundwater and 795 kg of sediment, assuming a sediment density of 2.65 g cm^{-1} and a porosity of 0.25 [8]. The model assumes homogenous plug flow with no dispersion or additional advection in the aquifer and therefore, only samples with little mixing, as indicated by $[Br]/[Br]_0 > 0.85$, were used for model fitting. Since injection was rapid (approximately 3 hrs), the rings were filled within minutes during the push phase. However, the time between "pulls" is large (from 1 to 24 hours), so the resting time was divided into 20 equal-sized time steps to have sufficiently small dt in eqs. 3 and 4 to account for reaction in each ring. The one-step model was evaluated using $x_f=1$. The best fit of parameters were achieved by minimizing the least square differences between the modelled concentrations and the measured total dissolved As concentration for the undiluted samples used for model. The first sampling point was ignored because the concentrations are changing so rapidly that small timing differences at this point significantly altered the fit of the other data. The sensitivity of model results to the box size was tested using a model with 10-fold smaller boxes (each box with 10 L of groundwater) and this did not substantially change results.

Groundwater Flow and Solute Transport Model

The 3D groundwater model was modified from the flow-only model of Michael and Voss [15-17] to include advective-dispersive transport. This added complexity enables simulation of solute concentrations, which are the values measured in groundwater and relevant for human health. Model geometry, shown in Figure S1, and flow boundary conditions (steady-state, prescribed head at the elevation of the land surface across the top of the model) are described in Michael and Voss [15,16]. Transport boundary conditions are C=1 in the top 1 m of the aquifer within the high-As area (Fig. S5) and C=0 in the top 1 m elsewhere. Initial concentration is C_0=1 within the top 50 m of the high-As area, C_0=0 elsewhere (Fig. S1), which is consistent with observations of As concentrations with depth, *e.g.* BGS and DPHE [8]. Sorption is modelled at depths below 94 m over most of the basin (in some areas, where permeable sediments are thin, this zone becomes shallower) with retardation factors of 1, 14.2, and 133.5. This is equivalent to equilibrium K_d values of 0, 1, and 10 L kg^{-1} assuming a porosity of 0.2 [16] and a bulk density of 2.65 g cm^{-3}, or K_d values of 1.3 and 13 L kg^{-1} assuming a bulk density of 2.00 g cm^{-3}. Longitudinal dispersivity was set to 100 m, consistent with literature values on the scale of vertical arsenic transport (150-200 m) [18, 19], horizontal transverse dispersivity was 0.1 m, and vertical transverse dispersivity was 0.01 m.

Supplementary Results

This section provides a comprehensive summary of additional data and experimental results that were used to assess As adsorption on the brown sediments as well as the flow and transport model of the Bengal Basin. The experimental site location and geochemical characteristics of the aquifer are described first. A summary of the adsorption experimental results is given next. This is followed by description of the flow and transport model and parameters used.

Characteristics of Groundwater and Sediment

The site of the sorption and push-pull experiments (90.6˚ E, 23.8˚ N), located 30 km east of Dhaka, has been described previously [20]. The deeper, brown aquifer has low concentrations of As, P, S, Mn and Fe, a near neutral pH and an alkalinity of approximately 8 mEq L^{-1} (Table S1). Groundwater chemistry was similar in the four wells screened between 55 and 59 m used in the brown adsorption experiments. Shallow groundwater from the gray sediments was obtained from a depth of 41 m and had a similar pH and sulphate content as the deeper groundwater. Groundwater As, Fe and P were higher, while groundwater Mn, alkalinity and conductivity were significantly lower.

The amount of As adsorbed or associated with amorphous Fe oxides on the sediment was assessed by sequential extraction. On the brown sediment, little As could be removed by desorption in distilled water, while 0.3 mg kg^{-1} was desorbed by 1M phosphate and an additional 0.8 mg kg^{-1} was removed with a warm, 1.2N HCl extraction (Table S2). Extractable As was greater and more variable in the gray sediment, with total extractable As ranging from 3.5 to 6.2 mg kg^{-1}. The drill cuttings are biased towards the larger grain sizes, as some of the clay and silt

particles are removed in the drilling process [21]. Grain size analysis of the cuttings indicated that they consisted of 87% sand, 11% silt and 2% clay by weight (Table S2), while core samples of a brown aquifer at nearby site showed a grain size distribution of 80% sand, 13% silt and 8% clay [22]. The cuttings from each depth had similar amounts of HCl-extractable Fe (10.7 and 10.8 g kg^{-1}, respectively). Again, the composition of the gray sediments were more variable, but were predominately sand and the HCl-extractable Fe ranged from 7.6 to 17.8 g kg^{-1}.

X-ray absorption near edge spectroscopy (XANES) was used identify Mn minerals present in the sediment. Most Mn was found in Mn^{2+} and Mn^{3+} minerals and little to no Mn^{4+} minerals were present (Figure S2).

The disperstivity of the aquifer was estimated by fitting the results of the bromide only push-pull test using the analytical solution proposed by Schroth *et al.*[13]. The initial low Br concentrations in the pull were due to the injection of an additional 80 L of groundwater without tracer, such a situation cannot be addressed with the analytical method and therefore the fit of the Br data from these early time points were not considered. The aquifer is assumed to have a porosity of 0.25 [8] and the radius of influence was calculated to be 73 cm. Best fit, determined by least squares, was achieved with a disperstivity of 0.5 cm (Figure S3). Over 90% of the injected Br was recovered when the volume removed during the pull equalled the volume injected ($V=V_0$) and 97% was recovered by the end of the experiment when $V= 1.5\ V_0$.

Adsorption Experiments: Estimating K

Batch isotherm (BI) experiments determined equilibrium partitioning (K) and capacity (S_{max}) for As(III) and As(V) in both brown and gray sediments (Table S3). Batch kinetic (BK)

experiment monitored As(III) adsorption kinetics over 400 hours (Table S4). Push-pull tests evaluated As(III) and As(V) adsorption *in situ* over 200 hours (Tables S5 and S6).

The BI experiments show that As(III) and As(V) adsorption onto brown sediment are non-linear and can be approximated by Langmuir isotherms (Figure 2). At environmentally relevant concentrations when solute [As] is < 3,000 μg L^{-1} (Table S3), over 90% of As were found to be adsorbed by the sediment. The amount of As adsorbed on the sediment was calculated from the loss in groundwater, while the initial adsorbed As was assumed to be negligible. The isotherm experiments were assumed to be at or near equilibrium. Using the Langmuir isotherm (eq. 1), K and S_{max} were determined to be 20 L kg^{-1} and 40,000 μg As kg^{-1} sediment, respectively, for both As(III) and As(V). Higher estimates of K were obtained when considering only samples spiked with <3,000 μg L^{-1} of As (29 and 49 L kg^{-1} for the As(III) and As(V) additions, respectively, Table S3). The K of the batch kinetic (BK) experiment was determined to be 68 L kg^{-1} for As(III) at 400 hours (Table S4). The slow kinetics of As adsorption likely resulted in the observed range of Ks in the batch experiment, as equilibrium may not have been reached in the BI experiments and this effect would be more pronounced with larger additions.

The batch experiments on shallow, gray sediment demonstrated a lower partitioning than observed in the brown sediments (Figure 2 and S4). Since saturation was not reached in these experiments, As adsorption can only be described using the partition coefficient, K_d. The K_d is approximately 1.5 L kg^{-1} in the three BI experiments, with no difference observed between As(III) and As(V). At 40 m, the K_d is 1.4±0.1 L kg^{-1} (r^2=0.95) and 1.6±0.1 L kg^{-1} (r^2=0.98) for As(III) and As(V), respectively, while at 46 m the K_d for As(III) is 1.1±0.1 L kg^{-1} (r^2=0.99).

Adsorption was more rapid in the gray sediment than the brown, with near complete adsorption by 5 hrs and a K_d of 1.1±0.2 L kg^{-1} (excluding the sample from 64 hrs, Table S4).

In the batch kinetic and push-pull experiments on brown sediments, As adsorption over time followed two- step kinetics, initially fast followed by a slower approach to equilibrium (Figure 1 and S5) [23-26]. The two-step kinetics of As adsorption may result from the slow diffusion to the interior surface sites that are less accessible. Groundwater As concentrations in the BK experiment of As(III) declined rapidly in the first 5 hours, and then at a slower rate between 5 and 400 hrs and was well described using the two-step model with 23% of the total As adsorption sites as readily available ("fast") sites (x_f) and 77% as slow sites (Figure S5). This proportion of fast sites is similar to other heterogeneous flood plain aquifers where interior space was estimated to comprise 70 to 90% of the total space available and was attributed to the presence of fine material, weathering and sand compaction [27-29]. Initially rapid and then slower As adsorption was also observed in the push-pull tests for As(III) and As(V) (Figure 1 and S6A). For the As(V) push-pull, 7 samples collected over 70 hours were relatively unaffected by dilution, defined as $[Br]/[Br]_0$ >0.85 (Table S5). As(V) was quickly adsorbed such that 80% of the injected [As(V)] (188 µg L^{-1}) was adsorbed in 6 hours, reaching a plateau of 90% (or 18 µg L^{-1}) by 45 hours. For the As(III) push-pull, 5 undiluted samples were collected over 48 hours (Table S6). As(III) adsorption was slower compared to As(V), with only 60% of injected [As(III)] (213 µg L^{-1}) to have been adsorbed in the first 6 hours, about 80% by 50 hrs and a plateau of 90% was reached at 145 hours once considerable dilution had occurred. In both tests, the loss of As was much faster than would have occurred from dilution alone. Dilution occurred more quickly in the As(III) experiment because less groundwater was injected than in the As(V) experiment. The dilution within the experiments was similar; when the volume removed by the

pull equalled the amount injected ($V=V_0$) the Br recovery was 75 and 76% for As(V) and As(III), respectively.

Parameter estimation in the push-pull experiments rely on the estimation of the equilibrium partitioning, [K, L kg^{-1}], capacity [S_{max}, µg kg^{-1}], adsorption (forward) reaction rate constant, [k_f, hr^{-1}], the fraction of fast to total sites [x_f, dimensionless] and the diffusion rate constant between the two types of sites [k_{diff}, hr^{-1}] and the equations used are included in the Supplementary Methods. The same groundwater [As] can be simulated, however, with multiple combinations of K and x_f values. Therefore, three different adsorption scenarios were considered (Figure 1 and Table S8). This process cannot identify a unique K for the aquifer sediments, but instead offers a plausible range of potential K values.

First, the conservative assumption that all adsorption sites are equal and readily accessible was used (one-step model, x_f= 100%) and this predicted the lowest K values (0.5 and 1.8 L kg^{-1} for As(III) and As(V), respectively, Table S8 and Figure 1). The modelled groundwater As concentrations, however, plateau too early and does not reflect concentrations observed in the later, diluted points. Second, the proportion of fast and slow sites (25 and 75%, respectively) from the batch kinetic experiment was used as an upper bound estimate of the availability of fast sites. This results in K's of 1.7 (r^2=0.96) and 5.1 (r^2=0.98) L kg^{-1} for As(III) and As(V), respectively. Third, the K value for As(V) determined in the batch isotherm experiment, 50 L kg^{-1}, was used to fit the other parameters (k_f, x_f and k_{diff}) for the As(V) push-pull test. The proportion of fast sites was estimated to be only 3% of the total adsorption sites. The x_f and k_{diff} from the As(V) experiment was then used to estimate K and k_f for As(III) since these factors are measures of the aquifer properties; best fits was achieved with a K value about 4-fold smaller (13 L kg^{-1}) and k_f value 2-fold slower than As(V) adsorption. In all models S_{max}

was set at 40,000 μg kg^{-1}, based on the batch isotherm experiments. The calculated diffusion rate is sufficiently slow that little As is transferred to the slow sites during the push phase (<5%), but during the pull phase As is steadily diffusing and becomes equally distributed in the two phases. It is also important to note the non-linear sensitivity of K to determination of fast adsorbing sites.

These results give a plausible range of adsorption that may be achieved and also illustrates that potential importance of both intra- and intergranular pore spaces in adsorption. The batch kinetic experiment estimated that 77% of adsorption sites were slower to adsorb. While we did not investigate the mechanisms controlling the difference in adsorption rates, one common explanation is intragranular porosity. In a similar sandy, quartz-based aquifer on Cape Cod, intragranular porosity was estimated to be 80% [27]. If the majority of the fast sites are located on the surface (while most slower sites are intragranular), it is obvious that access to many of the fast sites will become restricted in the compacted aquifer to the intergranular spaces, as compared to essentially infinite intergranular spaces for a well shaken slurry. Access to fast sites may also be restricted by transport of As along larger preferential flow paths during the rapid injection of the push, where groundwater penetrated over 1 m into the aquifer in 3 hours, while vertical recharge is estimated to be on the order of centimetres to meters per year in Bangladesh [30,31]. Should the injection of high-As water be slower, the modelled interior sites might become more comparable to the estimates of intragranualar porosity. Adsorption in the push-pull tests likely falls between the 2 estimates of fast sites (3% and 25% of all sites). The batch results should be considered a high-end estimate and may not be representative of the adsorption that will occur in the actual aquifer. As the kinetic analysis demonstrates, As adsorption on brown sediment is not instantaneous, but equilibrium is reached on the order of

days to weeks and this rate is rapid relative to the rate of natural groundwater flow. Therefore under natural flow conditions As adsorption should not be limited by kinetics and a larger partitioning could be expected.

Kinetic limitations, and therefore partitioning as low as 0.5 L kg^{-1}, may still be important in cases of well failure (where there is breakage of the pipe or flow along the casing). The rates of vertical groundwater flow in these scenarios are not known, but are presumably much faster. In Araihazar, the hydraulic head of deeper aquifer is typically 50 cm to 1 m lower than the shallow aquifer [22], thus considerable amounts of water could flow through a broken well casing. These point sources of As contamination could be a large source of As into the deeper aquifer and deserves further attention.

Adsorption Experiments: Further considerations

Arsenic speciation of the groundwater was measured in the batch isotherms and push-pull tests to assess potential differences in sorption of As species and to determine if significant oxidation or reduction was occurring. It has been suggested that only As(V) is effectively adsorbed on the brown sediment and As(III) adsorption is the result of its oxidization by Mn^{4+} oxides in the sediment and then adsorption as As(V) [32]. The isotherms for As(III) and As(V) at 58 m are very similar and there was no significant oxidation of the As(III) additions (Figure S7) suggesting no difference in sorption by As species. The voltammetry measurements are based on standard additions and require a high level of dilution, which also increases the error associated with these measurements. The samples for which the percent of As(III) is greater than 100% are regarded as containing only As(III), since the total As concentration is considered the more accurate measure of concentration. In the As(V) push-pull test, minor amounts (between 3 and 7 μg L^{-1}) of As(III) were detected using the Meng columns and were not considered to be

significant (Table S5). The As(III) injection had 13% As(V) during the injection phase and varied between 15 and 28% in the undiluted samples, however there was no trend over time (Table S6). It is unclear if there was indeed 13% As(V) in the injection solution, which seems unlikely, or if this ratio reflects a limitation of the columns' use in the field. Regardless, the lack of a trend in percent of As(III) do not support the idea of extensive As(III) oxidation. Insignificant amounts of Mn^{4+} oxides were identified using XANES and no other reactive minerals were found that would induce As oxidization on the sediment (Figure S2). These results suggest that while it is clear that As(III) adsorption is slower and can be significantly limited on shorter time scales, this does not result from the need for extensive As(III) oxidation or the lack of As(III) adsorption capacity on the sediment.

A variety of water parameters were measured during the push-pull experiments, even though the experiments were designed to minimize any differences between the source and receiving wells. In general there was good agreement between the dissolved constituents of the two wells (Table S1). The three properties that could have the largest influence on As chemistry are the dissolved oxygen, [Fe] and [P]. Low levels of dissolved oxygen were detectable in all wells, but were not correlated with [Fe] and [P] (Figure S6). In both experiments, [P] decreased from 0.6 to 0.4 mg L^{-1} reflecting the slight difference between the source and receiving wells. In the As(III) experiment the initial loss of P was slightly greater than would have been expected from mixing alone, but by later time points there was no net change in groundwater P. The injected groundwater [Fe] was lower than either receiving well and remained low, between 0.1 and 0.4 mg L^{-1}, during the experiment. Groundwater [Mn] reflected the slight differences between the receiving wells and, similar to the [P], there was initially a slight loss in Mn in the As(III) experiment, but this was not sustained over time. The pH was slightly higher in the

source well (7.3) than in the receiving wells (6.8) and pH decreased from 7.2 to about 7.0 over the course of the experiment and remained slightly elevated from what was expected based on mixing alone.

Adsorption is assumed to be reversible in the Langmuir isotherm and this was confirmed by the sequential extraction of sediments from the batch experiments (Table S3). Water alone was unable to remove much adsorbed As in 24 hrs suggesting that the kinetics of desorption are much slower than adsorption, as is commonly observed[11]. The following two steps (1M phosphate and warm, 1.2 N HCl) recovered 90 to 130% of the As adsorbed during the batch experiments. Most of the recovered As was removed in the phosphate extraction. A similar proportion, and not absolute amount, of As was then extracted by HCl regardless of size of the spike.

Groundwater Flow and Solute Transport Model

Simulations were run with three pumping scenarios, as described in the main text: split scheme ('S', irrigation pumping 50-100 m depth, domestic pumping 150-200 m depth) and deep scheme ('D', both domestic and irrigation pumping 150-200 m depth), with two domestic pumping rates for the split scheme, 50 L person^{-1} day^{-1} ('SC', estimated current rate, also used in the deep scheme) and 200 L person^{-1} day^{-1} ('SH', possible future rate with increased population and usage). K_d values of 0, 1, and 10 were simulated for each of the three pumping scenarios and are referred to as SC0, SC1, SC10 and so forth. Simulation results are shown in Figure 3 and S8. Though sorption provides some protection to the deep parts of the aquifer system, the deep pumping rate strongly affects the vulnerability of deep resources.

Additional simulations were run to assess the influence of vertical hydraulic conductivity on As breakthrough. The model base case [15] was a Kh:Kv of 10,000:1 in the split scenario with current pumping rates and a K_d of 1 L kg^{-1} (SC1) and additional runs increased the vertical conductivity, by decreasing the anisotropy to 1,000:1 and 100:1 for the SCI scenario; results are also shown in Table S9.

References

1 Gran, G. A new method to linearize titration curves. *Analyst* **77** (1952).

2 Meng, X. G., Korfiatis, G. P., Jing, C. Y. & Christodoulatos, C. Redox transformations of arsenic and iron in water treatment sludge during aging and TCLP extraction. *Environmental Science & Technology* **35**, 3476-3481 (2001).

3 Cheng, Z., Zheng, Y., Mortlock, R. & van Geen, A. Rapid multi-element analysis of groundwater by high-resolution inductively coupled plasma mass spectrometry. *Analytical and Bioanalytical Chemistry* **379**, 512-518 (2004).

4 He, Y., Zheng, Y., Ramnaraine, M. & Locke, D. C. Differential pulse cathodic stripping voltammetric speciation of trace level inorganic arsenic compounds in natural water samples. *Analytica Chimica Acta* **511**, 55-61 (2004).

5 Jung, H. B. & Zheng, Y. Enhanced recovery of arsenite sorbed onto synthetic oxides by L-ascorbic acid addition to phosphate solution: calibrating a sequential leaching method for the speciation analysis of arsenic in natural samples. *Water Research* **40**, 2168-2180 (2006).

6 USEPA. Method 300: Determination of Inorganic Anions by Ion Chromatography (eds Environmental Monitoring Systems Laboratory, Office of Research and Development, Cincinnati, OH, 1993).

7 Poppe, L. J., Hastings, P. & Polloni, C. USGS East Coast Sediment Analysis: Procedures, Database and Georeferenced Displays. *U.S. Geological Survey Open-File Report 00-358* (2000).

8 BGS/DPHE (British Geological Survey, Dept. of Public Health Engineering, Bangladesh). *Arsenic Contamination of Groundwater in Bangladesh, Final Report* (Keyworth, UK, 2001).

9 He, Y. & Zheng, Y. Assessment of in vivo bioaccessibility of arsenic in dietary rice by a mass balance approach. *Science of the Total Environment* **408**, 1430-1436, doi:10.1016/j.scitotenv.2009.12.043 (2010).

10 Quicksall, A. N., Bostick, B. C. & Sampson, M. L. Linking organic matter deposition and iron mineral transformations to groundwater arsenic levels in the Mekong delta, Cambodia. *Applied Geochemistry* **23**, 3088-3098, doi:10.1016/j.apgeochem.2008.06.027 (2008).

11 Limousin, G. *et al.* Sorption isotherms: A review on physical bases, modeling and measurement. *Applied Geochemistry* **22**, 249-275 (2007).

12 Wu, S. C. & Gschwend, P. M. Sorption Kinetics of Hydrophobic Organic- Compounds to Natural Sediments and Soils. *Environmental Science & Technology* **20**, 717-725 (1986).

13 Schroth, M. H., Istok, J. D. & Haggerty, R. In situ evaluation of solute retardation using single-well push-pull tests. *Advances in Water Resources* **24**, 105-117 (2001).

14 Cassiani, G., Burbery, L. F. & Giustiniani, M. A note on in situ estimates of sorption using push-pull tests. *Water Resources Research* **41**, W03005 (2005).

15 Michael, H. A. & Voss, C. I. Controls on groundwater flow in the Bengal Basin of India and Bangladesh: regional modeling analysis. *Hydrogeology Journal* **17**, 1561-1577, doi:10.1007/s10040-008-0429-4 (2009).

16 Michael, H. A. & Voss, C. I. Estimation of regional-scale groundwater flow properties in the Bengal Basin of India and Bangladesh. *Hydrogeology Journal* **17**, 1329-1346, doi:10.1007/s10040-009-0443-1 (2009).

17 Michael, H. A. & Voss, C. I. Controls on groundwater flow in the Bengal Basin of India and Bangladesh: regional modeling analysis. *Hydrogeology Journal* **17**, 1561-1577, doi:10.1007/s10040-008-0429-4 (2009).

18 Gelhar, L. W.,Welty, C. & Rehfeldt, K. R. A critical review of data on field-scale dispersion in aquifers. *Water Resources Research* **28**, 1955-1974 (1992).

19 Neuman, S. P. Universal scaling of hydraulic conductivities and dispersivities in geologic media. *Water Resources Research* **26**, 1749-1758 (1990).

20 Radloff, K. A. *et al.* Mobilization of arsenic during one-year incubations of gray aquifer sands from Araihazar, Bangladesh. *Environmental Science & Technology* **41**, 3639-3645 (2007).

21 Horneman, A. *et al.* Decoupling of As and Fe release to Bangladesh groundwater under reducing conditions. Part I: Evidence from sediment profiles. *Geochimica et Cosmochimica Acta* **68**, 3459-3473 (2004).

22 Zheng, Y. *et al.* Geochemical and hydrogeological contrasts between shallow and deeper aquifers in two villages of Araihazar, Bangladesh: Implications for deeper aquifers as drinking water sources. *Geochimica et Cosmochimica Acta* **69**, 5203-5218 (2005).

23 Fuller, C. C., Davis, J. A. & Waychunas, G. A. Surface-chemistry of Ferrihydrite. 2. Kinetics of arsenate adsorption and coprecipitation. *Geochimica et Cosmochimica Acta* **57**, 2271-2282 (1993).

24 Raven, K. P., Jain, A. & Loeppert, R. H. Arsenite and arsenate adsorption on ferrihydrite:

Kinetics, equilibrium, and adsorption envelopes. *Environmental Science & Technology* **32**, 344-349 (1998).

25 Selim, H. M. & Zhang, H. Arsenic adsorption in soils: Second-order and multireaction models. *Soil Science* **172**, 444-458 (2007).

26 Wu, S. C. & Gschwend, P. M. Sorption Kinetics of Hydrophobic Organic- Compounds to Natural Sediments and Soils. *Environmental Science & Technology* **20**, 717-725 (1986).

27 Wood, W. W., Kraemer, T. F. & Hearn, P. P. Intragranular diffusion - An important mechanism influencing solute transport in clastic aquifers. *Science* **247**, 1569-1572 (1990).

28 Harvey, C. F. & Gorelick, S. M. Rate-limited mass transfer or macrodispersion: Which dominates plume evolution at the Macrodispersion Experiment (MADE) site? *Water Resources Research* **36**, 637-650 (2000).

29 Haggerty, R. & Gorelick, S. M. Multiple-rate mass-transfer for modeling diffusion and surface-reactions in media with pore-scale heterogeneity. *Water Resources Research* **31**, 2383-2400 (1995).

30 Harvey, C. F. *et al.* Arsenic mobility and groundwater extraction in Bangladesh. *Science* **298**, 1602-1606 (2002).

31 Stute, M. *et al.* Hydrological control of As concentrations in Bangladesh groundwater. *Water Resources Research* **43** (2007).

32 Stollenwerk, K. G. *et al.* Arsenic attenuation by oxidized aquifer sediments in Bangladesh. *Science of the Total Environment* **379**, 133-150 (2007).

Supporting Tables

S1 Groundwater characteristics

S2 Sediment characteristics

S3 Batch isotherm experimental data

S4 Batch kinetic experimental data

S5 Push-pull data from the As(V) injection

S6 Push-pull data from the As(III) injection

S7 Push-pull data from the Br only injection

S8 Results of the As adsorption experiments

S9 Model results for one observation location and high-As area at approximately 160 m depth

Supporting Figures

S1 Model geometry, finite difference grid, and boundary and initial conditions for solute transport

S2 Mn speciation by X-ray absorption near edge spectroscopy (XANES)

S3 Br recovery over continuous pull with estimated disperstivity

S4 Batch isotherm results

S5 Batch kinetic results

S6 Groundwater constituents in the push-pull tests

S7 Speciation in the batch isotherms

S8 Areas of the deep low-As aquifer zones at risk of contamination, including simulations using K_d = 10 kg L^{-1}.

Table S1. Groundwater characteristics. The groundwater for the batch experiments was collected from I-1 for the brown sediments and I-2 for the gray sediments. The source water for both push-pull experiments came from I-4, while the receiving (rec.) wells were I-7 and I-9 for As(V) and As(III), respectively.

Well ID		I-1	I-4	I-7	I-9	I-2
Use		**Batch**	**Source**	**Rec. AsV**	**Rec. AsIII**	**Gray Batch**
Depth	m	55.9	59.7	57.9	58.5	41.1
pH		7.36	7.21	6.59	6.96	6.90
As	µg/L	2	2	1	2	210
AsIII	µg/L	2	2	1	1	200
P	mg/L	0.57	0.58	0.41	0.42	1.51
S	mg/L	0.05	0.09	0.33	0.07	0.14
Mn	µg/L	138	152	201	53	36
Fe	mg/L	0.40	0.59	0.53	0.15	3.31
Alkalinity	mEq/L	8.96	7.72	7.90	8.31	1.93
	+/-	0.21	0.31	0.28	0.32	0.05
Conductivity	mS/cm	1.18	0.92	1.13	1.20	0.07

Table S2. Sediment characteristics. Arsenic and Fe concentrations from the extraction of the sediment (drill cuttings) used in the batch experiments are shown as well as the relative grain sizes.

	Gray		Brown	
Extractions (mg/kg)	**40m**	**46m**	**55m**	**58m**
Water- ext As	0.03	0.39	0.00	0.00
Phosphate-ext As	1.10	1.92	0.37	0.28
HCl- ext As	2.37	3.86	0.68	0.88
Total Ext. As	3.50	6.17	1.05	1.16
Total Ext. Fe	17,790	7,580	10,650	10,820
Grain Size (% by weight)				
>150 µm	72.8	84.5	82.5	90.6
63-150 µm	20.5	7.7	14.2	7.8
<63 µm	6.7	7.8	3.3	1.6

Table S3. Batch isotherm experimental data. Compilation of the data collected for each bottle of the batch isotherm experiments, including total [As] and [As(III)], as well as the results from the desorption experiments. Samples from 55 and 58 m depth are brown sands, while the 40 and 46 m depth are gray sands from the high-As aquifer zone. Groundwater had 2.2 µg/L of As before additions to the brown sediments and 221 µg/L of As for the gray sediments. Dry weight was estimated for samples used in mineralogy analysis. Samples that were not analyzed are indicated with a 'na', while those with non-detectable concentrations are indicated by 'nd'.

					Dissolved As		Speciation		Ads. As	Extractions			
Experiment	**No.**	**GW**	**Sed.**	**pH**	**Initial**	**at 145 hrs**	**AsIII**	**% AsIII**	**at 145 hrs**	**Water**	**Phos.**	**HCl**	**Total**
		mL	g		µg/L	µg/L	µg/L		µg/kg	µg/kg	µg/kg	µg/kg	µg/kg
55m -AsIII	0	9.6	5.4	7.30	2	3	2	61%	-1	3	368	677	1,048
	1	9.6	5.4	7.31	445	37	26	70%	724	10	1,107	999	2,116
	3	9.6	5.3	7.34	888	44	nd		1,520	18	1,690	1,323	3,030
	5	9.6	5.5	7.31	1,773	306	643	210%	2,543	32	2,715	1,661	4,409
	7	9.6	5.0	7.30	3,544	619	198	32%	5,589	Sample for mineralogy			
58m -AsIII	0	9.6	4.7	7.31	2	1	nd		2	3	283	876	1,163
	1	9.6	5.6	7.40	445	38	69	182%	696	120	760	913	1,794
	2	9.6	4.8	7.33	666	18	nd		1,306	8	1,510	1,062	2,580
	3	9.6	4.7	7.34	888	34	nd		1,751	17	1,993	1,161	3,171
	4	9.6	5.3	7.39	1,330	76	121	159%	2,272	12	2,345	1,215	3,573
	5	9.6	5.6	7.40	1,773	141	236	167%	2,786	23	2,852	1,552	4,427
	6	9.6	5.6	7.37	2,658	163	141	87%	4,257	57	4,117	1,725	5,898
	7	9.6	7.2	7.47	3,544	318	368	116%	4,299	149	3,212	1,914	5,275
	8	9.6	5.3	na	7,086	728	na		11,548	453	10,012	3,358	13,822
	9	9.6	5.5	na	14,169	3,012	na		19,541	330	20,018	6,485	26,833
	10	9.6	5.0	na	28,336	10,306	na		34,847	Sample for mineralogy			
58m -AsV	1	9.6	3.9	7.40	502	22	na		1,179	16	1,624	1,028	2,668
	3	9.6	4.2	na	1,002	47	na		2,177	24	2,540	1,193	3,756
	5	9.6	4.7	7.36	2,002	89	na		3,878	27	3,901	1,420	5,348
	7	9.6	4.8	na	4,002	429	na		7,206	96	7,171	2,371	9,638
	8	9.6	5.4	na	8,002	1,158	na		12,169	90	11,198	3,505	14,793
	9	9.6	5.1	na	16,002	4,142	na		22,299	1,809	22,355	6,798	30,963
	10	9.6	5.0	na	32,002	12,641	na		37,079	Sample for mineralogy			
40m -AsIII	0	10	5.0	7.10	221	169	222	132%	105	26	1,096	2,374	3,496
	1	10	4.5	7.19	646	356	602	169%	644	4	2,190	2,412	4,606
	2	9.8	5.3	7.16	872	508	692	136%	671	33	2,249	2,945	5,227
	3	9.6	5.4	7.18	1,107	570	1,060	186%	957	26	1,916	2,523	4,466
	4	9.6	5.1	7.11	1,549	877	1,170	133%	1,266	193	1,751	3,334	5,278
	5	9.6	5.9	7.14	1,992	1,086	1,470	135%	1,480	65	1,870	2,309	4,245
	6	9.6	4.7	7.16	2,877	1,480	2,140	145%	2,833	179	4,158	3,565	7,903
	7	9.6	6.8	7.18	3,763	2,298	3,010	131%	2,617	Sample for mineralogy			
40m -AsV	1	9.6	5.3	7.21	721	461	456	99%	473	24	1,953	2,448	4,426
	4	9.6	5.6	6.93	1,721	820	1,410	172%	1,532	281	1,743	3,259	5,284
	5	9.6	4.5	6.67	2,221	1,391	2,600	187%	1,759	20	2,402	4,115	6,537
	7	9.6	4.3	7.20	4,221	2,361	4,070	172%	4,178	4	5,810	4,847	10,661
46m -AsIII	0	9.6	5.3	7.22	221	211	370	176%	19	387	1,917	3,862	6,166
	1	9.6	4.9	7.24	664	467	na		383	155	2,223	4,379	6,757
	3	9.6	4.3	7.24	1,107	714	863	121%	877	570	2,425	4,617	7,611
	5	9.6	5.5	7.28	1,992	1,192	na		1,388	458	2,113	3,988	6,559
	7	9.6	6.8	7.33	3,763	2,241	2,930	131%	2,546	Sample for mineralogy			

Table S4. Batch kinetic experimental data. As adsorption was monitored over 400 hrs. The experiment on brown sediments used 34.5 g (dry) sediment collected from drill cuttings at 58 m and 150 mL of groundwater from well I-1, while 49.2 g of gray sediments were collected at 40 m and 140 mL of groundwater from well I-2.

	Brown Sediment		Gray Sediment	
Time	**Dissolved As**	**Adsorbed As**	**Dissolved As**	**Adsorbed As**
hr	μg/L	μg/kg	μg/L	μg/kg
0	2,893	0	3,226	0
5	2,256	2,713	2,249	2,811
10	1,657	5,263	2,162	3,061
28	1,271	6,907	2,299	2,667
40	932	8,355	2,476	2,156
64	659	9,514	1,191	5,855
400	232	11,336	2,375	2,447

Table S5. Push-pull data from the As(V) injection. Compilation of the data collected during the As(V) push-pull experiment, which used water from well I-4, modified it with 190 µg/L of As and pushed it into well I-7. The pH and DO measurements and the As(III) column separation were conducted in the field, while samples for the other parameters were measured in the lab. The double line indicates when significant dilution began ($[Br]/[Br]_0 < 85\%$) and 'na' indicates samples that were not analyzed.

Sample	Time	Vol.	Br	As	AsIII	As III	P	S	Mn	Fe	DO kit	Alk.		pH
	hr	L	mg/L	µg/L	µg/L	%	mg/L	mg/L	µg/L	mg/L	ppm	meq/L	+/-	
Receiving well				2	2		0.41	0.33	201	0.53		7.90	0.28	6.59
Source well				1	1		0.58	0.09	152	0.59		7.72	0.31	7.21
Injection	3.0	1,240	40	189	0	0%	0.59	0.11	129	0.23	0.15	9.04	0.78	7.25
1	1.5	101	40	80	7	9%	0.58	0.08	167	0.36	0.25	8.95	1.37	7.25
2	3.5	204	39	56	6	11%	0.58	0.12	159	0.39	0.40			7.20
3	6.3	302	40	38	5	13%	0.56	0.10	152	0.16	0.25			7.35
4	12.4	399	37	32	6	20%	0.56	0.15	158	0.16	0.20			7.28
5	24.1	505	36	27	5	17%	0.55	0.19	158	0.21	0.20			6.96
6	44.5	607	37	18	4	22%	0.53	0.22	146	0.16	0.15	7.37	0.08	7.18
7	68.8	697	36	20	4	22%	0.54	0.24	157	0.27	0.15			7.07
8	92.8	783	32	17	3	18%	0.51	0.16	161	0.35	0.25			7.17
9	116.5	872	22	16	3	20%	0.55	0.20	159	0.26	0.15			7.04
10	142.0	961	17	13	4	30%	0.52	0.21	162	0.29	0.06			6.71
11	166.3	1,049	17	na	na	na	na	na	na	na	0.10			7.01
12	189.0	1,136	6	12	4	31%	0.51	0.32	185	0.33	0.40			7.24
13	213.9	1,236	4	11	4	34%	0.47	0.27	173	0.26	0.20			6.80
14	214.8	1,354	2	8	3	37%	0.50	0.27	159	0.21	0.10			
15	215.5	1,440	1	8	2	27%	0.43	0.21	139	0.16	0.20			7.01
16	216.2	1,536	na	na	na	na	na	na	na	na	0.30			
17	217.0	1,634	na	na	na	na	na	na	na	na	0.20			7.01
18	217.8	1,737	na	7	na	na	0.43	0.17	120	0.15	0.40			
19	218.8	1,836	na	na	na	na	na	na	na	na	0.15			6.89
20	219.8	1,942	na	na	na	na	na	na	na	na	0.15			6.88
21	220.3	2,045	na	6	2	37%	0.40	0.14	112	0.11	0.10			6.90

Table S6. Push-pull data from the As(III) injection. Compilation of the data collected during the As(III) push-pull experiment, which used water from well I-4, modified it with 215 µg/L of As and pushed it into well I-9. The pH and DO measurements and the As(III) column separation were conducted in the field, while samples for the other parameters were measured in the lab. The double line indicates when significant dilution began ($[Br]/[Br]_0 < 85\%$) and 'na' indicates samples that were not analyzed.

Sample	Time	Vol.	Br	As	AsIII	As III	P	S	Mn	Fe	DO kit	Alk.		pH
	hr	L	mg/L	µg/L	µg/L	%	mg/L	mg/L	µg/L	mg/L	ppm	meq/L	+/-	
Receiving well				2	1		0.42	0.07	53	0.15		6.90	0.22	6.78
Source well				1	1		0.58	0.09	152	0.59		7.72	0.31	7.21
Injection	2.6	783	56	213	186	87%	0.57	0.07	120	0.20	0.02	7.35	0.28	7.19
1	1.9	112	58	127	105	83%	0.54	0.07	94	0.15	0.60	7.76	0.14	7.00
2	4.1	215	56	112	94	84%	0.58	0.06	83	0.08	0.40			7.22
3	6.0	313	54	88	74	85%	0.53	0.07	79	0.54	0.40			7.19
4	23.8	429	57	66	48	72%	0.49	0.06	67	0.07		7.00	0.33	7.13
5	47.6	548	48	49	35	72%	0.50	0.11	64	0.09	0.70			7.15
6	71.8	632	31	40	32	82%	0.50	0.06	64	0.09	0.25			7.03
7	95.1	729	19	32	27	86%	0.45	0.06	64	0.11	0.15			6.97
8	120.7	828	9	31	27	87%	0.47	0.05	69	0.19	0.20			6.91
9	144.8	931	3	26	21	82%	0.44	0.10	67	0.16	0.20			6.93
10	167.4	1,018	2	25	19	77%	0.43	0.06	64	0.15	0.25			7.20
11	190.9	1,171	1	19	15	79%	0.43	0.05	52	0.11	0.10			7.06
12	216.6	1,273	1	19	15	79%	0.44	0.09	56	0.13	0.15			6.81
13	217.1	1,371	1	18	13	75%	0.43	0.08	48	0.10	0.15			
14	217.5	1,471	1	na	na	na	na	na	na	na	0.10			6.90
15	218.0	1,571	na	13	9	76%	0.44	0.06	39	0.08	0.10			
16	218.5	1,673	na	na	na	na	na	na	na	na	na			7
17	219.0	1,774	na	na	na	na	na	na	na	na	0.35			
18	219.5	1,880	na	10	8	81%	0.39	0.07	32	0.04	0.10			6.92
19	219.9	1,974	na	na	na	na	na	na	na	na	0.15			
20	220.4	2,071	na	na	na	na	na	na	na	na	0.10			6.96
21	221.0	2,172	na	8	6	72%	0.41	0.07	30	0.05	0.15			6.90

Table S7. Push-pull data from the Br only injection. Compilation of the data collected during the Br only push-pull experiment, where 540 L of water from well I-1 was modified with 130 mg/L of Br and pushed it into well I-3. This injection was followed by another 80 L of unaltered water from I-1. After two days, the water was continuously withdrawn. Volume and Br concentrations are presented with the cumulative amount of Br removed.

Sample	Volume	Br	Cumulative Br
	L	mg/L	mg
Receiving well			
Source well			
Injection	540 +80	130	75.7
1	3	2.5	0.00
2	16	2.8	0.03
3	30	5.5	0.1
4	48	19.5	0.4
5	69	52.3	1.3
6	85	79.0	2.1
7	94	91.7	2.9
8	103	106.4	3.8
9	122	117.7	6.0
10	138	122.1	8.2
11	159	128.4	10.9
12	179	123.8	13.6
13	191	127.5	15.4
14	204	130.8	17.4
15	243	129.8	22.8
16	280	125.6	28.0
17	313	126.1	32.3
18	350	130.8	37.4
19	380	128.4	41.7
20	416	126.6	46.4
21	465	121.6	52.5
22	514	113.1	58.0
23	548	104.1	61.6
24	580	88.1	64.3
25	618	73.8	66.9
26	649	56.9	68.5
27	685	43.8	70.2
28	732	28.2	72.0
29	776	18.8	72.7
30	819	12.2	73.1
31	866	7.5	73.3
32	907	6.2	73.5

Table S8. Results of the As adsorption experiments on brown sediments. Equilibrium partitioning and capacity (K and S_{max}) were determined in the batch isotherm experiments. K was also estimated for a lower range of As concentrations (<3,000 µg/L). Using the S_{max} from the batch isotherms, K and the kinetic parameters (x_e, k_f and k_{diff}) were determined in the batch kinetic experiment. For the push-pull experiments, kinetic parameters were estimated using the range of Ks (30, 50 and 70) estimated from the batch experiments and suggest that only 2 to 5% of the adsorption sites were exposed. K from the push-pull experiments was also estimated using a x_e measured in similar aquifers (x_e = 20%) and assuming single porosity (100%).

		Batch Isotherms						Batch Kinetic	
		Additions up to 32,000			**Additions less than 3,000**			**AsIII**	
		55m- AsIII	**58m - AsIII**	**58m- AsV**	**55m- AsIII**	**58m - AsIII**	**58m- AsV**	**One Site**	**Two Site**
K	L/kg	14.7	19.9	20.1	12.8	28.7	48.6	68	68
S_{max}	µg/kg		40,000	40,000	40,000*	40,000*	40,000*	40,000*	40,000*
x_f	%	--	--	--	--	--	--	100%*	23%
k_f	1/hr	--	--	--	--	--	--	0.05	0.3
k_{diff}	1/hr	--	--	--	--	--	--	--	0.006
r^2		0.97	0.99	0.98	0.82	0.84	1.00	0.85	0.99

-- parameter not needed

* parameter set based on other experiment

		Push Pull					
		AsV			**AsIII**		
		One Site	**Two Site**		**One Site**	**Two Site**	
			Set x_f	**Set K**		**Set x_f**	**Set K**
K	L/kg	1.8	5.1	50	0.5	1.7	12.8
S_{max}	µg/kg	40,000*	40,000*	40,000*	40,000*	40,000*	40,000*
x_f	%	100%	25%	3%	100%	25%	3%
k_f	1/hr	0.4	1.8	16.0	0.2	0.7	7.5
k_{diff}	1/hr	--	4.30E-03	3.38E-04	--	1.00E-03	3.00E-04
r^2		0.87	0.98	0.97	0.94	0.96	0.99

-- parameter not needed

* parameter set based on other experiment

Table S9. Model results for one observation location and high-As area at approximately 160 m depth*. Time before breakthrough of 10% of initial [As] and normalize concentration at a time of 1,000 years are given for observation location shown in Fig. 2. Vulnerable area defined as percent of the high-As area with normalized [As] greater than 10% of initial [As] is given for 1,000 y and 5,000 y simulation times.

Pumping Scheme	Domestic Pumping Rate	K_d	Kh:Kv	Observation Location (Fig. 2)		Vulnerable Area (%) within High-As Area	
				Years until C/C_0=0.1	C/C_0 at 1,000 y	1,000 y	5,000 y
	[L/p-day]	[L/kg]					
Split	50	0	Base	526	0.79	56	70
Split	50	1	Base	>5,000	0	1	29
Split	50	10	Base	>5,000	0	0	0
Split	200	0	Base	143	1	84	85
Split	200	1	Base	1204	0.05	9	81
Split	200	10	Base	>5,000	0	0	2
Deep	50	0	Base	70	1	92	92
Deep	50	1	Base	570	0.36	63	92
Deep	50	10	Base	4950	0	4	41
Decreased Anisotrophy/ Increased Vertical Conductivity							
Split	50	1	1,000:1			11	57
Split	50	1	100:1			48	69

*The depth of the center of the uppermost finite-difference cell in the deep pumping zone is 162 m. In some areas, primarily outside of the high-As area, this depth is shallower due to thinning of basin sediments.

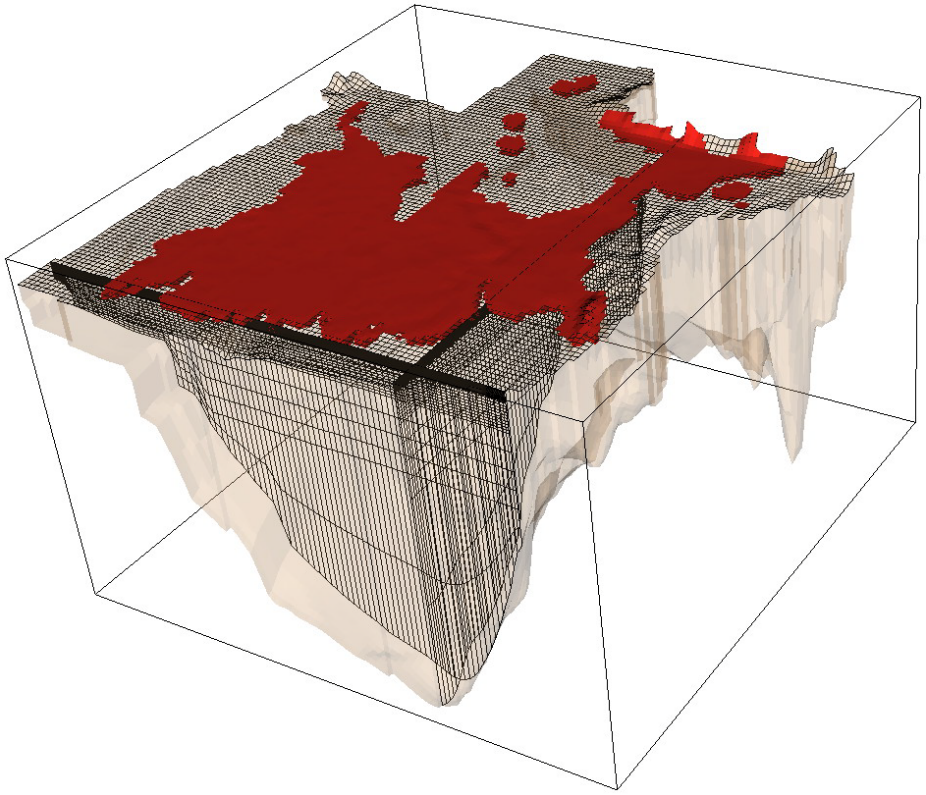

Figure S1. Model geometry, finite difference grid, and boundary and initial conditions for solute transport (red: C=1, no color: C=0). Vertical exaggeration is 100:1.

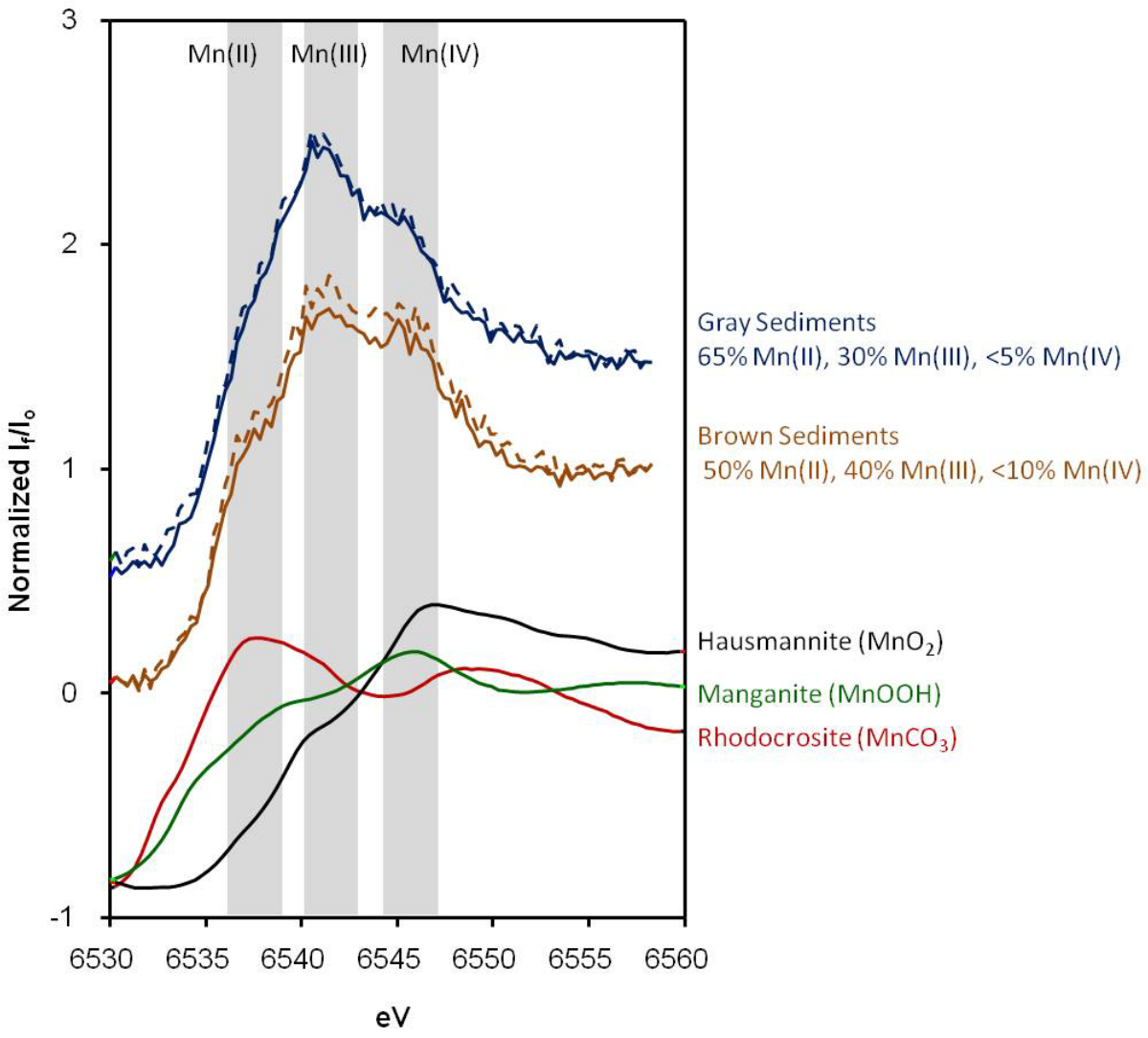

Figure S2. Mn speciation by X-ray absorption near edge spectroscopy (XANES). Measured spectra from the gray (40 m depth) and brown (58 m) sediments this site are shown along with three Mn reference minerals. Fits of the sediment spectra were produced by linear combination (dashed lines). Mn minerals in the sediments at both depths are predominately Mn(II) with a smaller contribution of Mn(III) minerals, while less than 10% of the Mn is present as Mn(IV).

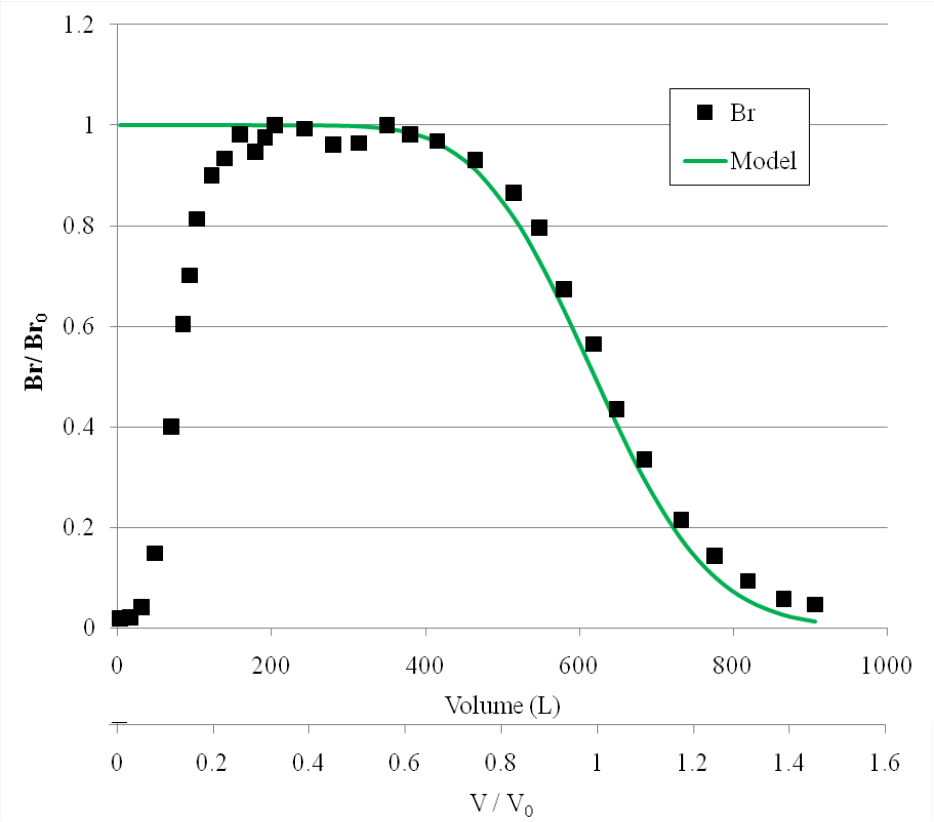

Figure S3. Br recovery over continuous pull with estimated disperstivity. Measured Br concnetrations from the tracer only push-pull were used to estimate aquifer disperstivity using the method described in Schroth, 2001. This test injected 540 L of water modified with 130 mg/L of Br followed by another 80 L of unaltered water. After two days, the water was continuously withdrawn. The model fit shown is with a disperstivity of 0.5 cm for the estimated 73 cm radius of influence for this push-pull test.

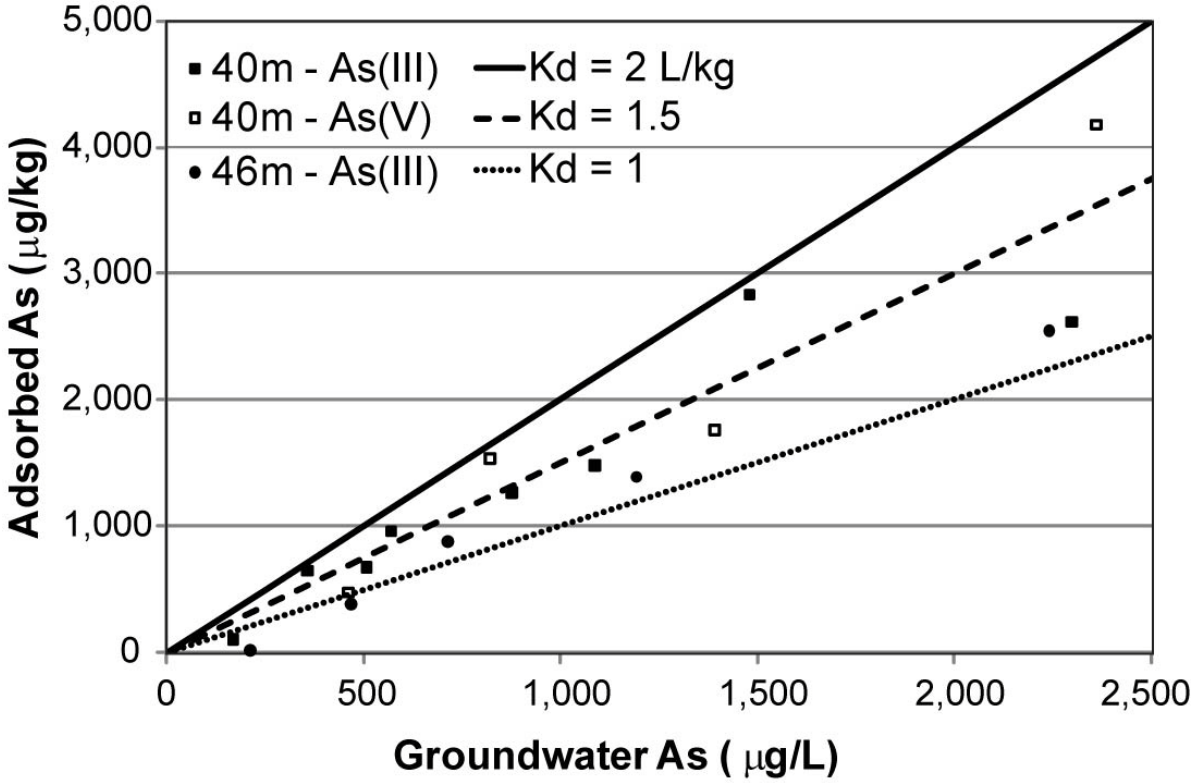

Figure S4. Batch isotherm experiments. Groundwater spiked with As(III) or As(V) was mixed with cuttings from the gray aquifers and sampled 145 hours later. Saturation was not reached on the gray sediments, therefore the partitioning coefficient, Kd, was estimated to be 1.5 L/kg.

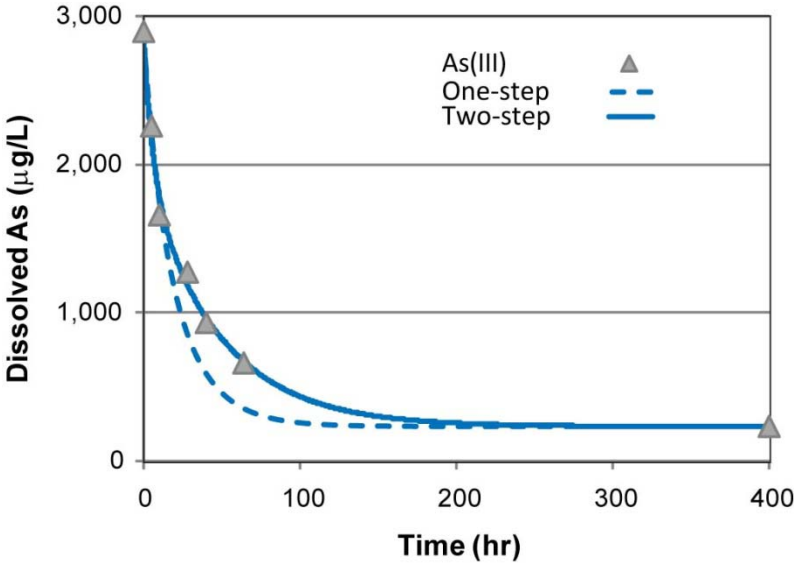

Figure S5. Batch kinetic results. Adsorption of spiked As(III) was observed over 400 hours on brown sediment collected at 58 m and had a K of 68 L/kg. Kinetic data was modeled using either the single or two-step models.

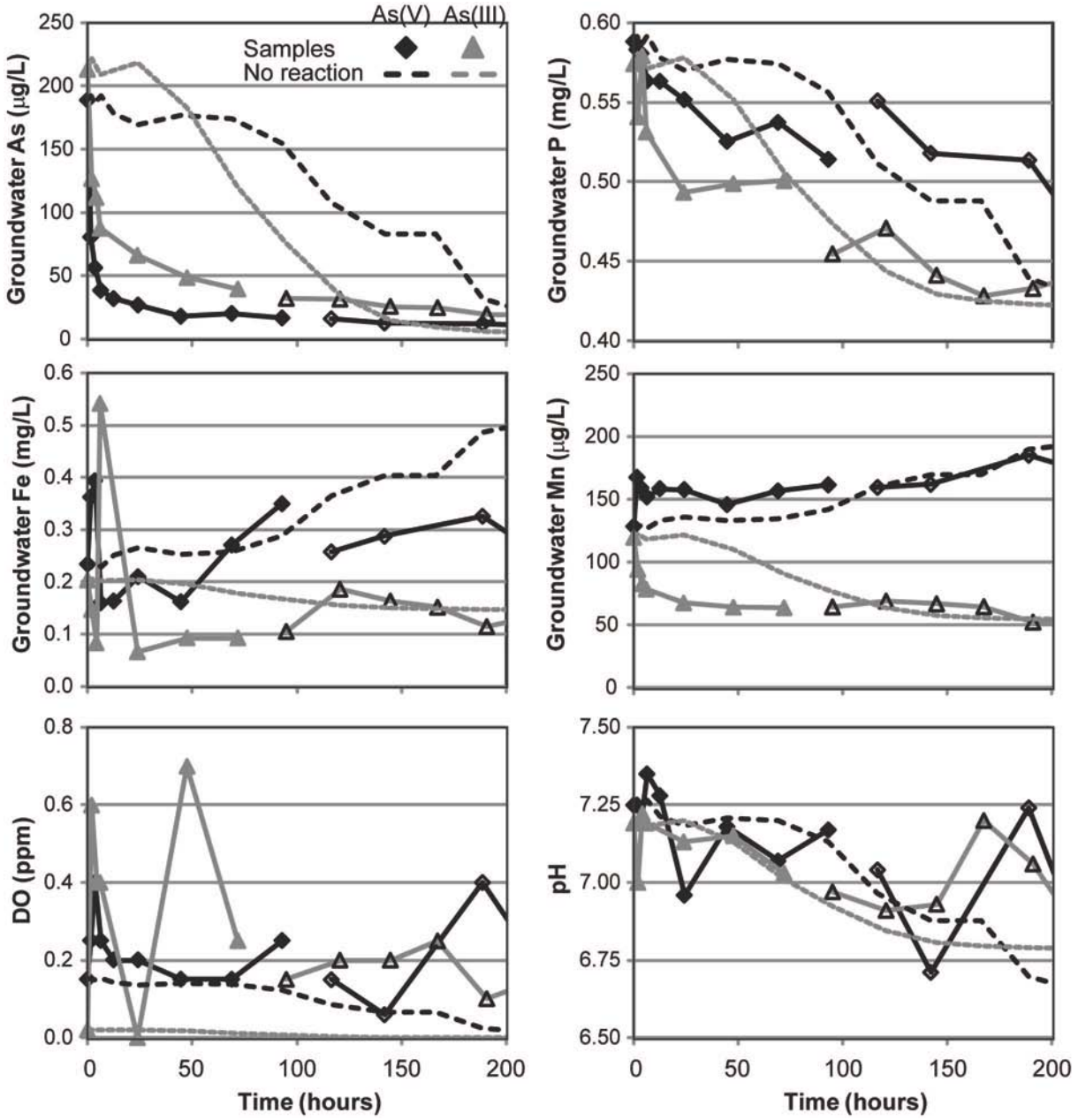

Figure S6. Push-pull results. Concentrations of As, P, Fe and Mn are shown as well as DO and pH. Results from the As(V) (black diamonds) and As(III) (gray triangles) push-pull tests are shown, with filled symbols indicating samples before significant Br dilution ($[Br]/[Br]_0 > 85\%$). The dashed lines indicate the expected concentrations if no reaction had occurred and are based on the concentrations in the source and receiving wells and [Br].

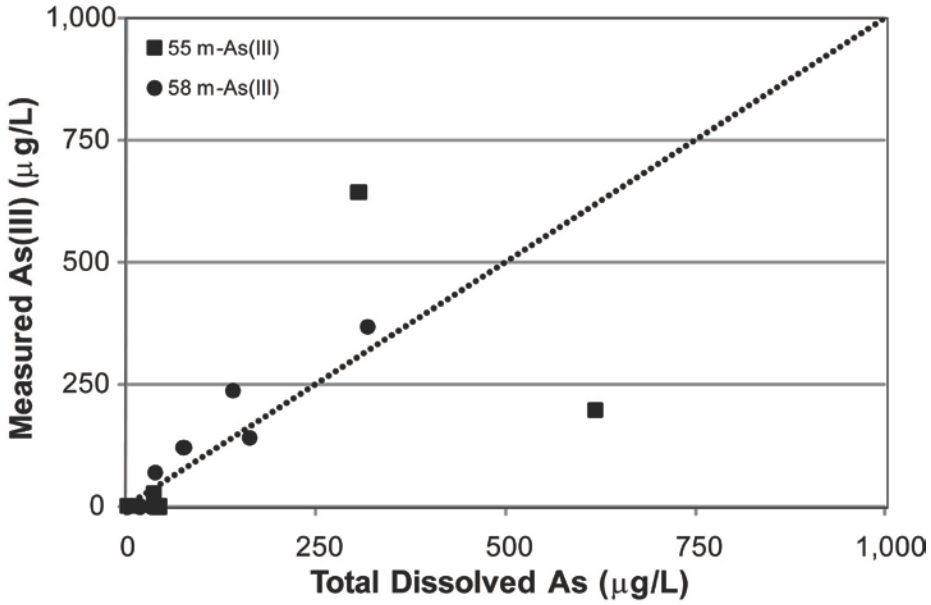

Figure S7. Speciation of supernatant As in batch isotherm experiments. Groundwater As speciation was measured by voltammetry when the samples were collected. Results suggest that spiked As(III) remained as As(III) in solution; the dashed line indicates when total groundwater As is completely As(III).

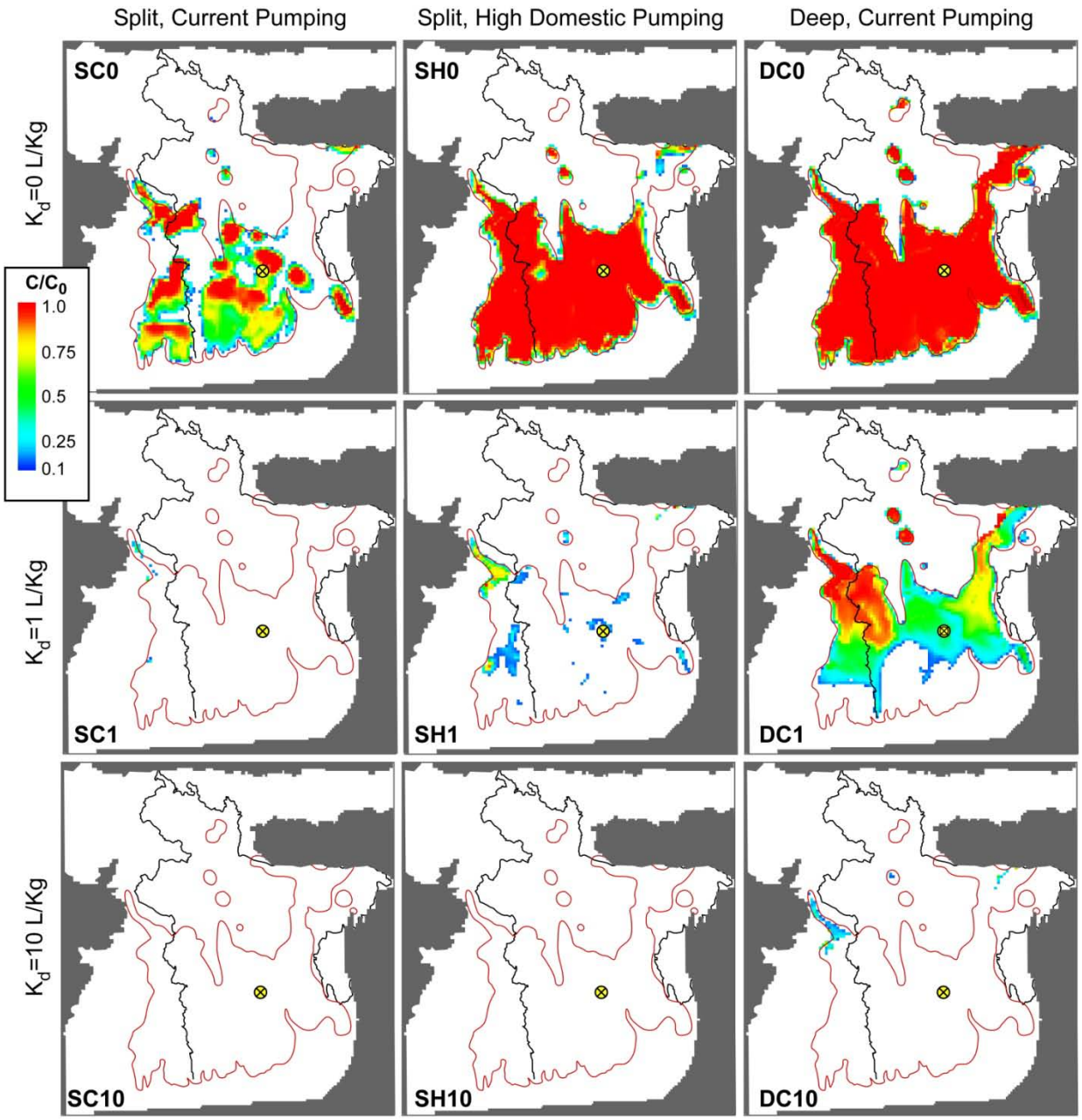

Figure S8. Areas of the deep low-As aquifer zones at risk of contamination, including simulations using K_d = 10 kg L^{-1}. Model boundary is enclosed in gray. Black line indicates the Bangladesh border and the red lines encircle the regions with high-As groundwater in the shallow aquifer zones (*2, 13*). The color scale indicates simulated [As] for C/C_0 >0.1 after 1,000 yr at a depth of 162 m below ground surface. Modeled [As] is shown for the 3 water use scenarios (SC, SH and D) - current 'split' with shallow irrigation and deep domestic pumping at 50 L day^{-1} $person^{-1}$ (SC), future 'split' with domestic use increased to 200 L/day-person (SH) and 'deep' pumping where both irrigation and current domestic use occurs in the deeper aquifer zone (DC) - and for no (K_d = 0 kg L^{-1}), low (K_d =1) and high retardation (K_d =10) for each scenario. The yellow dot indicates the location of plotted concentrations in Fig. 3.